NEUROPHYSIOLOGY

Chromatin-based reprogramming of a courtship regulator by concurrent pheromone perception and hormone signaling

Songhui Zhao[1]*, Bryson Deanhardt[2]*, George Thomas Barlow[1], Paulina Guerra Schleske[1], Anthony M. Rossi[3], Pelin C. Volkan[1,2†]

To increase fitness, animals use both internal and external states to coordinate reproductive behaviors. The molecular mechanisms underlying this coordination remain unknown. Here, we focused on pheromone-sensing *Drosophila* Or47b neurons, which exhibit age- and social experience–dependent increase in pheromone responses and courtship advantage in males. Fruitless^{M} (Fru^{M}), a master regulator of male courtship behaviors, drives the effects of social experience and age on Or47b neuron responses and function. We show that simultaneous exposure to social experience and age-specific juvenile hormone (JH) induces chromatin-based reprogramming of *fru^{M}* expression in Or47b neurons. Group housing and JH signaling increase *fru^{M}* expression in Or47b neurons and active chromatin marks at *fru^{M}* promoter. Conversely, social isolation or loss of JH signaling decreases *fru^{M}* expression and increases repressive marks around *fru^{M}* promoter. Our results suggest that *fru^{M}* promoter integrates coincident hormone and pheromone signals driving chromatin-based changes in expression and ultimately neuronal and behavioral plasticity.

INTRODUCTION

Animals tightly control social behaviors based on internal and external states, as inappropriate and untimely displays of these behaviors can interfere with reproductive success. Integration of signals such as age, reproductive state, and population density determines decisions regarding execution of specific social behaviors. Hormones act as critical signals for internal states such as age and reproductive state, which have long-lasting effects on the structure and behavioral outputs of neural circuits when coordinated with sensory experience (*1*). For example, female mice execute opposing social behaviors toward males using cyclic regulation of sensory neuron responses by female hormones (*2*). Recent studies also show that the critical period for social reward learning in adult mice requires both neural activity and oxytocin (*3*). Many circuits and behaviors are constrained by critical periods where they rely on sensory experience early in life for maturation of circuit structure and behaviors (*4*). Despite the overwhelming evidence that hormones synergize with sensory experience to reprogram social and reproductive behaviors, how these are coordinated at the molecular level remains unknown or poorly characterized.

To address this question, we used neural circuits driving courtship behavior in *Drosophila melanogaster*, which are under the control of a master transcriptional regulator Fruitless^{M} (Fru^{M}) (*5*, *6*). Fru^{M} is necessary and sufficient for male courtship behavior and is expressed in approximately 2000 interconnected neurons forming the courtship circuitry (*6*, *7*). Fru^{M} regulates development, function, and plasticity in circuits driving male-specific behaviors (*7*). Social cues such as pheromones can modulate courtship behaviors, some of which are detected by two classes of *fru^{M}*-positive olfactory receptor neurons (ORNs) expressing Or67d and Or47b receptors (*8*, *9*). Or67d neurons mediate male-male repulsion through detection of the male-specific pheromone cis-vaccenyl acetate (*8*). On the other hand, Or47b neurons detects fatty acid pheromones, such as palmitoleic acid (PA), present on both sexes, and function to increase the male courtship advantage with age (*9*–*12*). Recent studies showed that social context, juvenile hormone (JH) signaling, an age-related cue, and Fru^{M} co-regulate pheromone responses of Or47b neurons and age-related increase in courtship advantage (*10*). However, the molecular mechanisms regulating these changes remain unknown. We previously showed that genetic perturbations to Or47b function, calcium signaling, and the histone acetyltransferase p300/CBP (CREB–binding protein) regulate maintenance, but not onset, of *fru^{M}* expression in adult Or47b neurons (*13*). These results suggested the possibility that age and social environment can fine-tune neuronal sensitivity and courtship advantage through chromatin-mediated changes in Fru^{M} transcription and function.

Social experience enhances *fru^{M}* expression in Or47b neurons via chromatin-based mechanisms

To test whether social context regulates chromatin around *fru^{M}* promoter, we performed chromatin immunoprecipitations from male whole-antennae samples using antibodies against actively transcribed chromatin, followed by quantitative polymerase chain reaction (ChIP-qPCR). Association of RNA polymerase II with promoters and increase in acetylation of histones such as histone 3 lysine 27 (H3K27) and H3K9 are hallmarks of actively transcribed chromatin (*14*). ChIP-qPCR for *fruitless^{M}* transcriptional start site (TSS), showed dynamic changes in chromatin around *fruitless* P1 promoter with age. In group-housed (GH) male antennae, we found that RNA polymerase II and acetylated H3K27 (H3K27ac) enrichment around *fru* P1 promoter TSS are initially high at 0 to 2 days but decrease by day 5 (Fig. 1A). This is followed by an increase at 5 to 7 days, a peak time for sexual maturity for males (Fig. 1A). As opposed to the group house condition, single-housed (SH) socially isolated males showed a decrease in the enrichment of RNA polymerase II and H3K27ac at the *fru* P1 promoter across time (Fig. 1A). The effect of social isolation on

[1]Department of Biology, Duke University, Durham, NC 27708, USA. [2]Department of Neurobiology, Duke University, Durham, NC 27708, USA. [3]Department of Biology, New York University, New York, NY 10003, USA.
*These authors contributed equally to this work.
†Corresponding author. Email: pelin.volkan@duke.edu

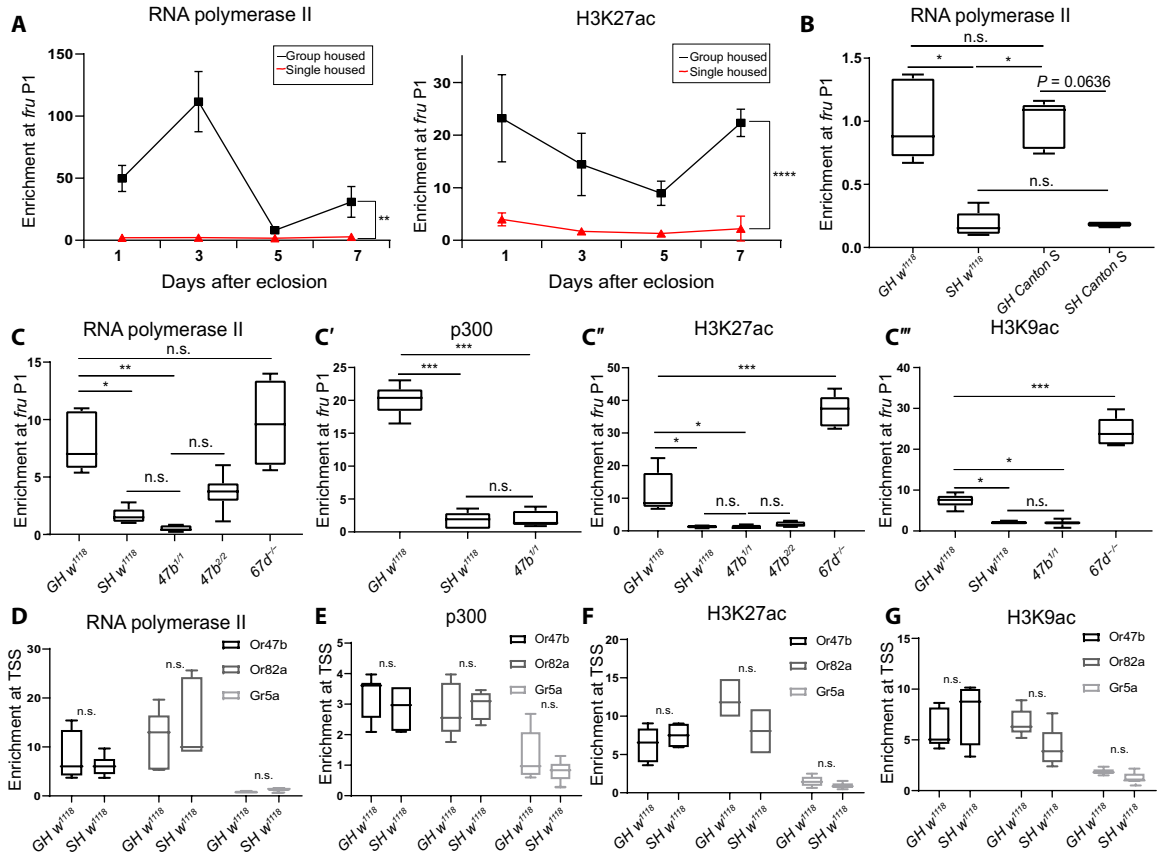

Fig. 1. Social experience increases open chromatin marks around *fru* P1 promoter. Antennal ChIP qPCR to measure association of open chromatin marks around *fru* P1 promoter using anti-RNA polymerase II, anti-H3K27ac, anti-H3K9ac, and anti-p300 antibodies from adult male antennal samples that are either GH (black) or SH (red) (A to C). *y* axis shows enrichment relative to no antibody control. Social isolation decreases enrichment of either mark in SH male antennae at all time points. (**A**) Time course of RNA polymerase II (left) and H3K27ac (right) association with *fru* P1 at days 1, 3, 5, and 7 after eclosion. (**B**) Enrichment of RNA polymerase II around *fru* P1 in 5-day-old GH and SH *Canton S* versus w^{1118} males. Enrichment of RNA polymerase II (**C**), p300 (**C′**), H3K27ac (**C″**), and H3K9ac (**C‴**) open chromatin marks around *fru* P1 are shown for GH and SH w^{1118}, *Or47b*, and *Or67d* mutants. (**D** to **G**) Enrichment of active chromatin marks (RNA polymerase II, p300, H3K27ac, and H3K9ac) upstream of genes expressed in the antenna (*Or82a* and *Or47b*) and not expressed in the antennae (*Gr5a*) in different housing conditions. *P < 0.05; **P < 0.005; ***P < 0.001; n.s., not significant.

chromatin was similar between different wild-type strains Canton S and w^{1118}, ruling out variation due to genetic background (Fig. 1B). Acetylation of both H3K27 and H3K9 are mediated by histone acetyltransferase p300/CBP Nejire (nej) (*15*, *16*). Consistent with this, we detected a decrease in the enrichment of p300/CBP and H3K9ac at *fru* P1 promoter in 5-day-old SH males (Fig. 1, C′ and C‴). As predicted, GH *Or47b* mutant males ($Or47b^1$ and $Or47b^2$) showed a decrease in enrichment of all marks examined (Fig. 1, C to C‴). In contrast, GH *Or67d* mutants ($Or67d^{[GAL4]}$), which previously were reported to have no effect on fru^M expression, showed no difference in RNA polymerase II enrichment from GH condition. However, an increase in H3K27ac and H3K9ac enrichment at *fru* P1 was observed in GH *Or67d* mutants compared to wild type (Fig. 1, C and C″) (*13*). This result points to possible increase in *fru* P1 open chromatin state in *Or67d* mutants that has not been previously reported. Relative enrichment was not significantly altered around antennal *Or47b* and *Or82a* promoters in GH or socially isolated male antennae (Fig. 1, D to G). In addition, enrichment of active chromatin marks was minimal around gustatory receptor *Gr5a* promoter, which shows little to no expression in the antennae based on previous antennal RNA sequencing analysis (Fig. 1, D to G) (*17*). These results suggest that social experience through Or47b signaling increases active chromatin marks around *fru* P1 promoter in sensory neurons.

To test whether social context-dependent changes in chromatin lead to changes in fru^M expression in Or47b and Or67d neurons, we quantified fru^{P1GAL4}-driven *UAS-GFP* expression using *40xUAS-mCD8::GFP* in 2-, 5-, and 7-day-old GH and SH male antennae (Fig. 2, A to C). Quantification of integrated green fluorescent protein (GFP) density in each ORN driven by fru^{P1GAL4}-driven *UAS-GFP expression* showed that in GH males, fru^M expression is initially low in both Or47b and Or67d ORNs and increases by days 5 to 7 (Fig. 2, A to C). Social isolation decreased the fru^{P1GAL4}-driven *UAS-GFP* expression in Or47b neurons but not in Or67d neurons at days 5 and 7 (Fig. 2, A to C). Quantitative reverse transcription PCR (qRT-PCR) on antennal samples also showed similar changes in endogenous fru^M expression in different ages and social context (Fig. 2D). The changes in social isolation are not too drastic at the transcriptional level compared to the differences seen at the chromatin level. Although this is unexpected, others have reported similar phenomena (*18*). These differences might indicate other unexplored chromatin-based effects on gene regulation such as changes in alternative splicing or transcriptional state (poised promoters versus transcriptional elongation) determined by the phosphorylation state of RNA polymerase II.

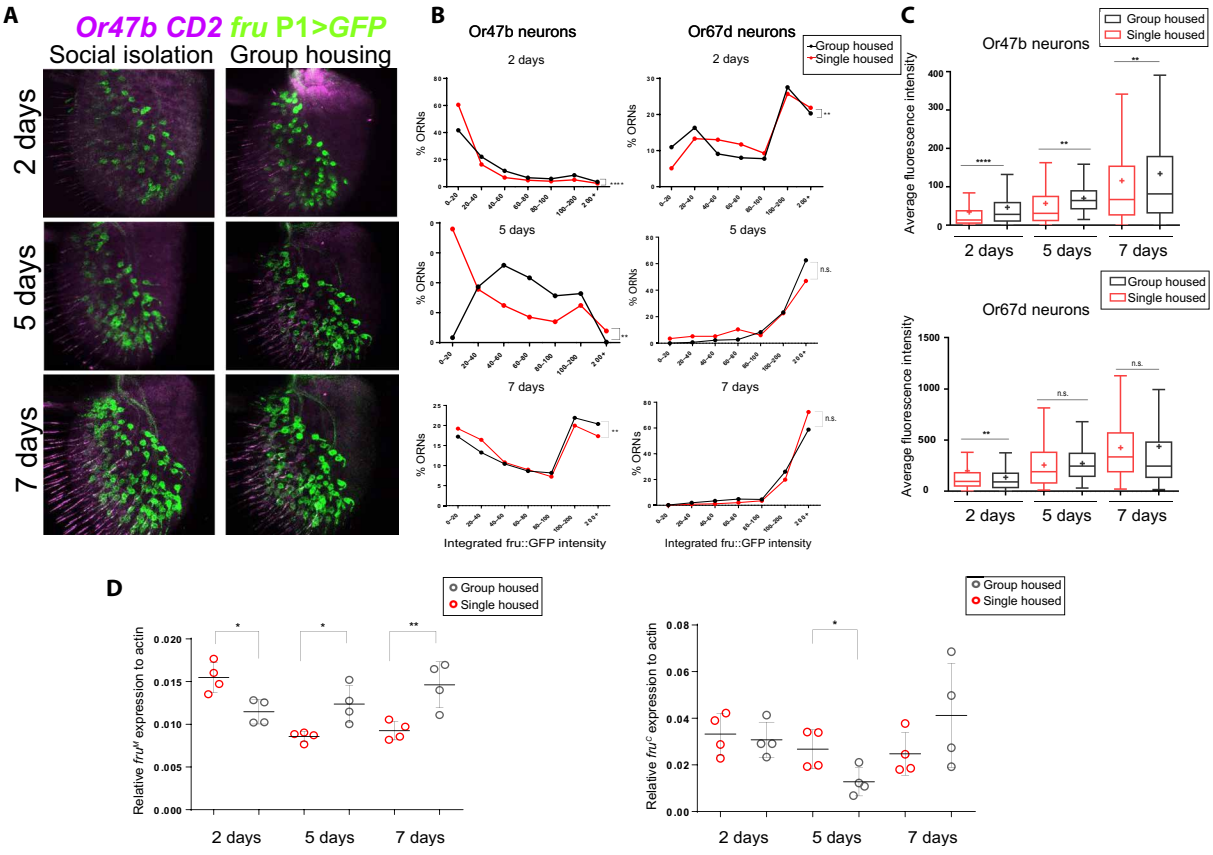

Fig. 2. Effects of social experience on *fru* expression. (**A**) Confocal images of fru^{P1GAL4}-driven *UAS-GFP* in the antennae from GH and SH males of different ages. (**B**) Quantification of fru^{P1GAL4}-driven *UAS-GFP expression* in Or47b and Or67d ORNs from (A). *x* axis shows integrated *GFP* density, and *y* axis represents the percent ORNs. (**C**) Average of the data points from (B). (**D**) qRT-PCR for fru^{M} (left) and fru^{C} (right) from antennal samples of w^{1118} males that are either SH or GH. $^{*}P < 0.05$; $^{**}P < 0.005$; $^{***}P < 0.001$.

Quantification of GFP and galactose-induced transcription factor (GAL4) transcripts from fru^{P1GAL4}-driven *UAS-GFP* flies also showed comparable changes in GFP expression between GH and SH males, thus making it an appropriate readout of fru^{M} transcription (fig. S1). Expression of olfactory receptors (ORs) (*Or47b*, *Or65a*, and *Or13a*) and housekeeping genes did not show a significant change in response to social isolation in males (fig. S1). These results suggest that social experience opens chromatin around *fru* P1, whereas social isolation decreases these active chromatin marks.

Pheromone and social exposure of isolated males open chromatin and rescue fru^{M} expression in Or47b neurons

Given that (i) Fru^{M} expression in Or47b neurons requires a functional Or47b receptor (*13*) and (ii) group housing increases fru^{M} expression, we reasoned that pheromone exposure or regroup housing may enhance fru^{M} expression in Or47b neurons. To test this hypothesis, we asked whether the decrease in fru^{M} expression seen in socially isolated males can be rescued by regrouping or exposure to Or47b ligand PA. In addition, we wanted to determine the effect of age and duration of the social exposure on fru^{M} expression and chromatin state. We transferred socially isolated males to vials containing 4.5 mg of PA starting days 0, 2, or 3 after eclosion and quantified fru^{P1GAL4}-driven *UAS-GFP* expression at days 5 and 7 (Fig. 3, A to F). We found that PA exposure rescues the fru^{M} expression to GH levels if exposed at day 0 in Or47b, but not Or67d ORNs, albeit levels of rescue depended on the length of exposure (Fig. 3, A to C). For example, exposing socially isolated males to PA from 3 to 5 days does not rescue the fru^{M} expression to GH level; however, 3- to 7-day exposure does (Fig. 3, D to F). In Or67d neurons, PA exposure at day 3 and taken to 7 days also showed significant effects in fru^{M} expression not seen in GH flies.

Given the amount of tissue required to perform ChIP, we proceeded with a naturalistic paradigm of regrouping flies in groups of 30 rather than exposing them to PA. In agreement with an increase in fru^{P1GAL4}-driven *UAS-GFP*, active chromatin marks also showed increased enrichment when socially isolated flies are regrouped starting at different ages for 7 days, yet the level of rescue was lower if flies were regrouped for a shorter period of 5 days (Fig. 3, G and H). The rate of rescue was comparable among flies grouped for similar durations, suggesting the absence of a critical period for social experience to modulate fru^{M} expression. Overall, these results show that the duration of exposure to PA or regrouping, at any age, is sufficient to rescue chromatin-based increase in fru^{M} expression.

Calcium signaling induces p300 association with *fru* P1 promoter and facilitates open chromatin

We next sought to determine the cellular signaling mechanisms downstream of Or47b that regulate fru^{M} transcription and chromatin around *fru* P1. *Drosophila* ORs are ion channels that conduct calcium and sodium (*19*). In response to increase in calcium from membrane receptors, calcium/calmodulin-dependent protein kinase I (CaMKI) is activated and phosphorylates p300/CBP (*20*).

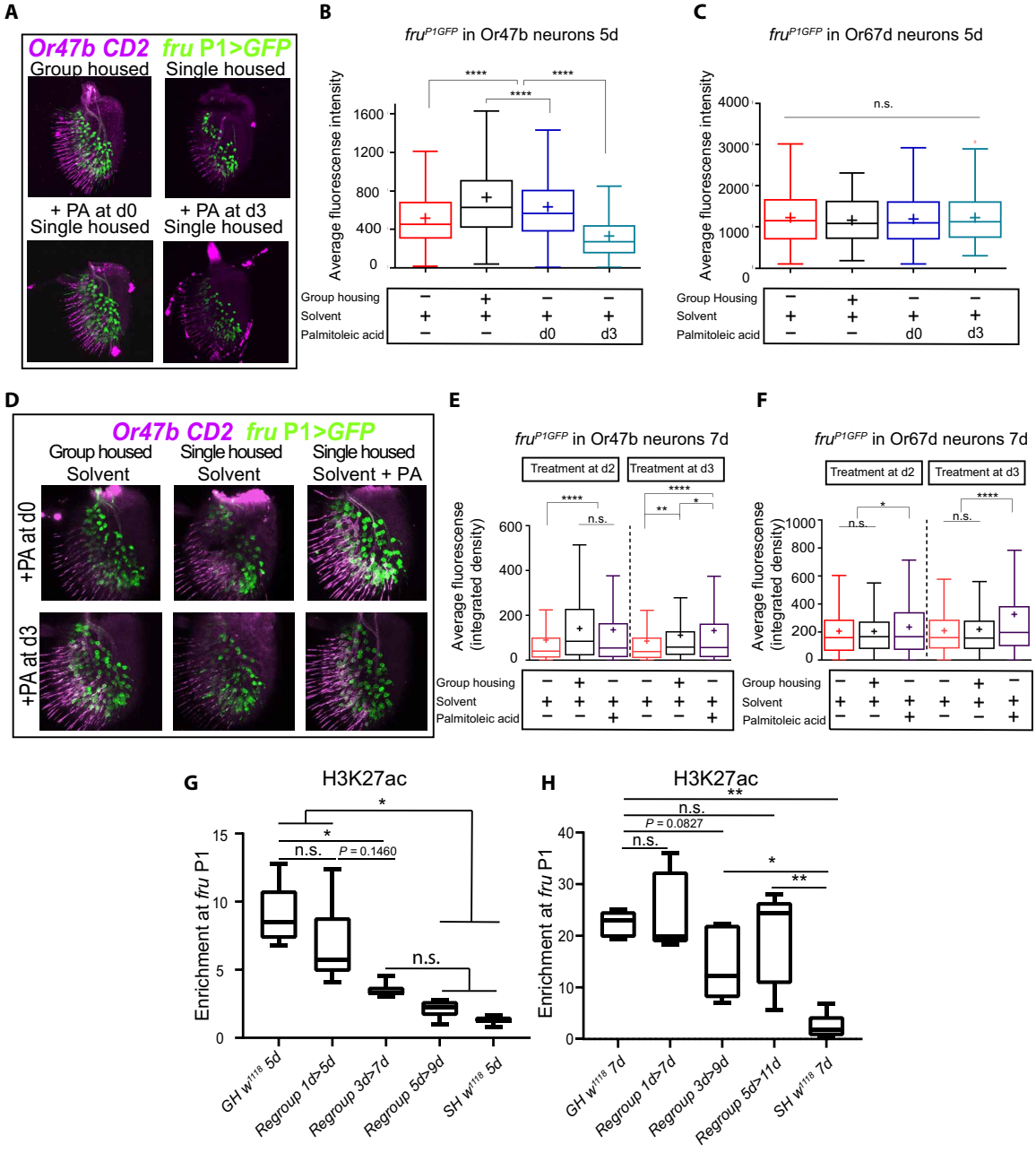

Fig. 3. Pheromone exposure and regrouping rescues chromatin-based effects around *fru* P1. *fru*^{P1GAL4}-driven *UAS-GFP* expression in male antennae from GH (top left) and SH (top right). Lower panels show *fru*^{P1GAL4}-driven *UAS-GFP expression* in SH males exposed to Or47b ligand PA between 0 to 5 or 3 to 5 days after eclosion (**A**) and 0 to 7 or 3 to 7 days after eclosion (**D**). Quantification of integrated GFP density from Or47b ORNs (**B**) and Or67d ORNs (**C**) in response to group housing, single housing, and 0 to 5 or 3 to 5 days of exposure of SH males to solvent or PA. Quantification of integrated GFP density from Or47b ORNs (**E**) and Or67d ORNs (**F**) in response to group housing, single housing, and 2 to 7 or 3 to 7 days of exposure of SH males to solvent or PA. (**G**) H3K27ac enrichment around *fru P1* in *w*^{1118} male antennae socially isolated and then regrouped for a duration of 5 days (1 to 5, 3 to 7, and 5 to 9 days after eclosion) compared to SH male antennae. (**H**) H3K27ac enrichment around *fru* P1 in *w*^{1118} male antennae socially isolated and then regrouped for a duration of 7 days (1 to 7, 3 to 9, and 5 to 11 days after eclosion) compared to SH male antennae. **P* < 0.05; ***P* < 0.005; ****P* < 0.001; *****P* < 0.0001; n.s., not significant.

This results in the activation of p300/CBP and leads to its association with transcription factors at the promoters of genes (*20*), which is followed by acetylation of histones, such as H3K9 and H3K27, and recruitment of RNA polymerase II to the promoters facilitating open active chromatin (*15*, *21*). In a previous study, we showed that calcium signaling from Or47b receptor is required to maintain the expression of *fru*^{M} in Or47b neurons (*13*). Knocking down CaMKI and its phosphorylation target histone acetyltransferase p300/CBP in *fru*^{M}-positive olfactory neurons deceases *fru*^{M} expression in Or47b neurons (*13*). These RNA interference (RNAi) knockdowns also exhibit defects in Or47b neuron sensitivity and age- and social experience–dependent courtship competition (*10*).

We predicted that in *Drosophila*, social experience–dependent changes in the fru^M expression can be due to chromatin-based changes induced around *fru* P1 promoter. Enrichment of p300 at *fru* P1 TSS increased with group housing and decreased in response to social isolation and in *Or47b* mutants (Fig. 1C′). As with RNA Pol II enrichment, p300, and its associated marks H3K9ac and H3K27ac, show no significant difference at *Or47b* or *Or82a* promoters in different social housing conditions (Fig. 1, D to G). To examine the contribution of both P300 and CaMKI to chromatin remodeling around fru^M, we used Or47b ORN–specific *CaMKI* and *p300-RNAi* knockdowns. Both RNAi knockdowns led to a decrease in RNA polymerase II, p300, H3K27ac, and H3K9ac enrichment at *fru* P1 TSS, suggesting that p300 association with the promoter requires CaMKI activity (Fig. 4, A to D). Enrichment at promoters of control *Or* genes were not affected in RNAi conditions. One exception to this is the enrichment of some of the acetylation marks around *Or47b* TSS in *Or47b-GAL4*–driven *p300-RNAi* knockdown, likely due to the fundamental role of p300 in transcription regulation. Although we cannot make any direct inferences for how p300 affects the chromatin around *Or47b*, it does inform us of the cell type specificity of our knockdown (fig. S2). Collectively, these data suggest that CaMKI signaling in response to social experience elevates fru^M transcription in Or47b neurons via p300-based chromatin modulation.

JH signaling regulates fru^M expression in Or47b neurons

Recent studies showed that JH signaling, which relays age-related information, enhances social experience–dependent increase in Or47b odor responses and courtship advantage (*22*). One molecular mechanism that can account for the age-dependent differences in neuronal responses and behavior is whether JH signaling regulates fru^M expression to modulate neuronal function. To test this hypothesis, we used RNAi-based knockdown of two putative JH receptors, *met* and *gce*, in either Or47b neurons or all fru^M-positive neurons. RNAi knockdown of both genes in fru^M-positive neurons resulted in a decrease in the expression of fru^{P1GAL4}-driven *UAS-GFP* expression (Fig. 5, A and B). fru^{P1GAL4}-mediated knockdown of *gce* and *met* decreased fru^M expression in both Or47b and Or67d neurons by day 7 (Fig. 5, A and B), albeit with more marked effects in Or47b ORNs, which might account for differences in fru^M regulation in different ORN population (Fig. 5, A and B).

We next analyzed open chromatin marks around *fru* P1 TSS in GH *met* and *gce-RNAi* knockdowns. Or47b neuron–specific RNAi knockdown of *met* and *gce* showed a decreased enrichment of RNA polymerase II at *fru* P1 TSS (Fig. 5C). Enrichment of p300 and H3K27ac was also dampened in these RNAi knockdowns. These results, together with the effects of social isolation, suggest that the stabilization of active chromatin marks around *fru* P1 promoter requires both JH signaling and social experience.

Time course of JH regulation of fru^M expression in ORNs

Previous studies have revealed that JH signaling in the first 3 days of life is responsible for the critical period of courtship learning and maturation in *Drosophila* (*23*). This period overlaps with JH titers, which peak at eclosion and decrease after 2 to 3 days into adulthood (*24*). Given the requirement for both group housing and JH signaling in stabilizing active chromatin marks around *fru* P1, we predicted that the disruption of JH receptor function in the first 2 to 3 days after eclosion could have different effects on fru^M expression. Previous studies have shown that performing GAL4-driven RNAi knockdown experiments at different temperatures can modify RNAi effects, where

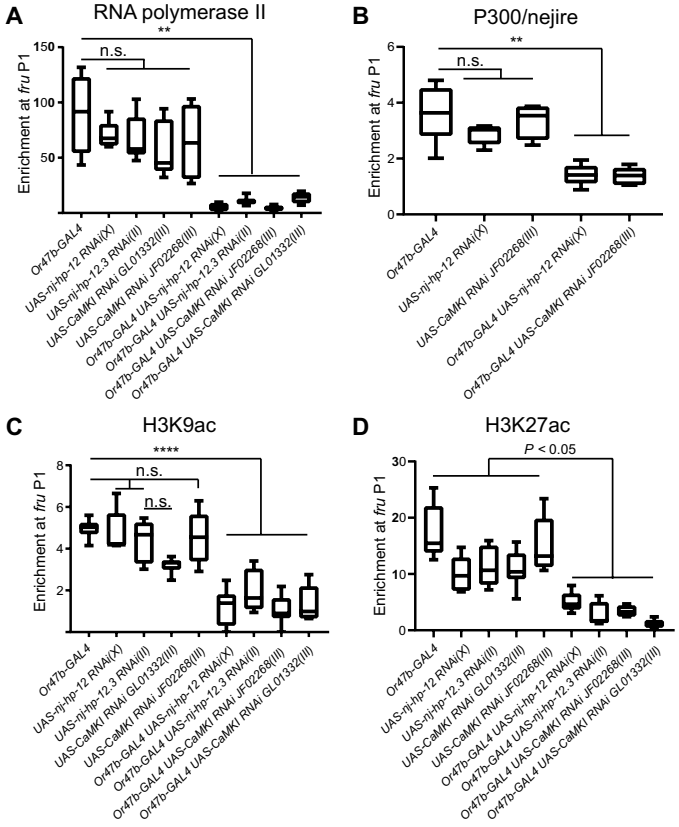

Fig. 4. Calcium signaling and p300 function in Or47b neurons facilitates active chromatin around *fru* P1. Enrichment of RNA polymerase II (**A**), p300 (**B**), H3K27ac (**C**), and H3K9ac (**D**) around *fru* P1 in GH male antennae in *Or47b-GAL4, UAS-CaMKI RNAi, UAS-nej (p300) RNAi, Or47b-GAL4 UAS-CaMKI RNAi*, and *Or47b-GAL4 UAS-nej (p300) RNAi*. Multiple *UAS-RNAi* lines were used for each gene indicated by the chromosome and stock name. $^{**}P < 0.005$; $^{****}P < 0.0001$; n.s., not significant.

lower temperatures weaken and, at times, completely rescue knockdown phenotypes (*25*, *26*). Given that fru^{GAL4}-mediated *met* and *gce* RNAi knockdown phenotypes are highly penetrant at 28°C, we probed fru^M expression in experiments where we restricted the knockdown to specific days by performing temperature shifts. Restricting *met* and *gce* RNAi knockdowns to development by switching temperature, the flies were raised from 28° to 22°C at eclosion resulted in an elevated fru^M expression compared to wild type (Fig. 5, D to F) (see Materials and Methods). This suggests that in pupal stages, JH receptors might act as repressors of *fru*. Performing the temperature shifts in successive days gradually reversed this trend in both neurons, where by day 7, flies transferred on day 3 appeared wild type and flies kept at 28°C for the entire experiment showed a significant decrease in fru^M expression in both ORN populations. This trend was true for fru^M expression in both Or47b and Or67d neurons, with a slower rate in the latter (Fig. 5, E and F). These results suggest that JH receptors possibly act as repressors of fru^M transcription in late pupal and early adult stages of life and switch to an activator after day 3 in the presence of social experience.

JH and pheromone signaling co-regulates chromatin to enhance fru^M expression in Or47b neurons

Information about the social environment via pheromone-sensing Or47b neurons and age-related internal states through JH signaling

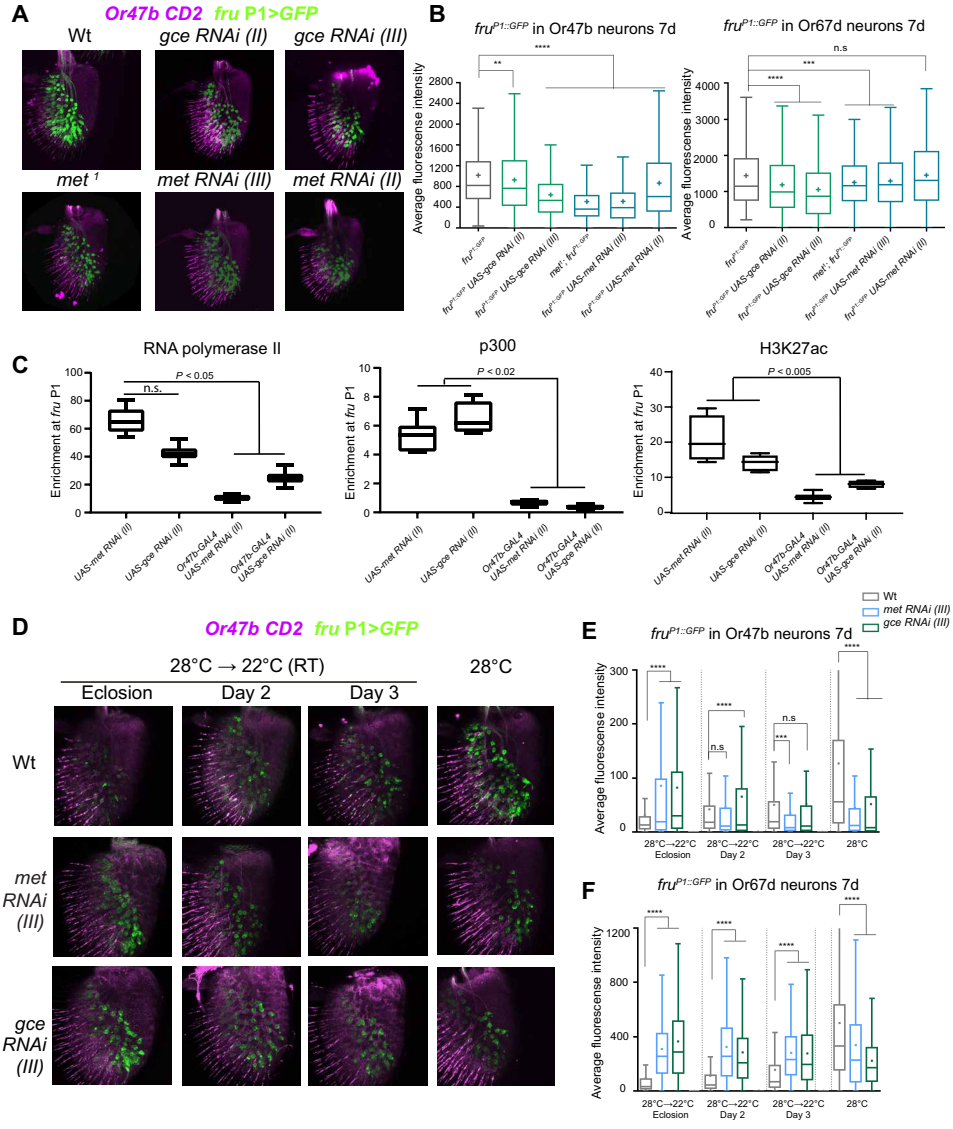

Fig. 5. JH signaling recruits transcriptional machinery and facilitates open chromatin at *fru* P1. (**A**) fru^{P1GAL4}-driven *UAS-GFP* expression in GH male antennae in *gce-RNAi* and *met-RNAi* knockdowns, as well as met^{1} mutants. *UAS-RNAi* expression is driven by fru^{P1GAL4}. (**B**) Quantification of GFP intensity from fru^{P1GAL4}-driven *40XUAS-CD8GFP* expression in Or47b and Or67d neurons from (A). (**C**) Enrichment of RNA polymerase II, p300, and H3K27ac at *fru* P1 in GH male antennae with genotypes *UAS-met RNAi*, *UAS-gce RNAi*, *Or47b-GAL4 UAS-met RNAi*, and *Or47b-GAL4 UAS-gce RNAi*. (**D**) fru^{P1GAL4}-driven *40XUAS-CD8GFP* expression in GH male antennae in *gce-RNAi* and *met-RNAi* knockdowns raised at 28° or 22°C to vary knockdown efficiency. The flies are either raised at 28°C for 7 days or transferred to 22°C at day 1, 2, or 3 after eclosion before GFP analysis on day 7. RT, room temperature; Wt, wild type. (**E** and **F**) Quantification of integrated GFP density of antennae in (D). ****$P < 0.0001$; n.s., not significant.

can synergize to modulate fru^{M} expression, neuronal sensitivity, and courtship advantage. But how do hormone and pheromone signals synergize to exert these effects on fru^{M} regulation at the molecular level? One possible mechanism of interaction would be whether JH receptor binding upstream of *fru* establishes a permissive or poised chromatin state around *fru* P1, which is stabilized by timely social experience, through p300 activity to regulate fru^{M} expression and function. Nuclear hormone receptors can directly interact with p300/CBP to regulate gene expression in mammals (*21*, *27*), and a conserved JH response element *CACACGCGAAAA* (E-box) exists 7721 base pairs upstream of *fru* P1. Thus, we hypothesized that JH receptors can interact with *fru* P1 TSS and E-box to regulate chromatin and fru^{M} expression in ORNs. To test whether JH receptors associate with E-box and *fru* P1 promoter, we performed ChIP from GH and SH male antennae using Gce antibodies followed by qPCR. These experiments showed that Gce is enriched at *fru* P1 in 5-day-old GH flies, and this association is dampened in response to *gce* RNAi knockdown in Or47b ORNs, demonstrating antibody specificity (Fig. 6A). Despite the significant decrease association of RNA Pol II and active chromatin marks in response to social isolation, we observe an age-dependent increase in Gce accumulation at both *fru* P1 promoter and E-box upstream of *fru* P1 in SH males (Fig. 6, B and C). Disrupting Or47b signaling can recapitulate the social isolation–dependent increase in Gce enrichment at both *fru* P1 and the E-box in Or47b neuron–specific knockdown of *CaMKI* and *p300-RNAi* (Fig. 6, D and E). Enrichment of Gce was not significantly different around another Gce-regulated gene *Kr-h1* in different social conditions and RNAi knockdowns, except for *p300* knockdown (figs. S3 and S4).

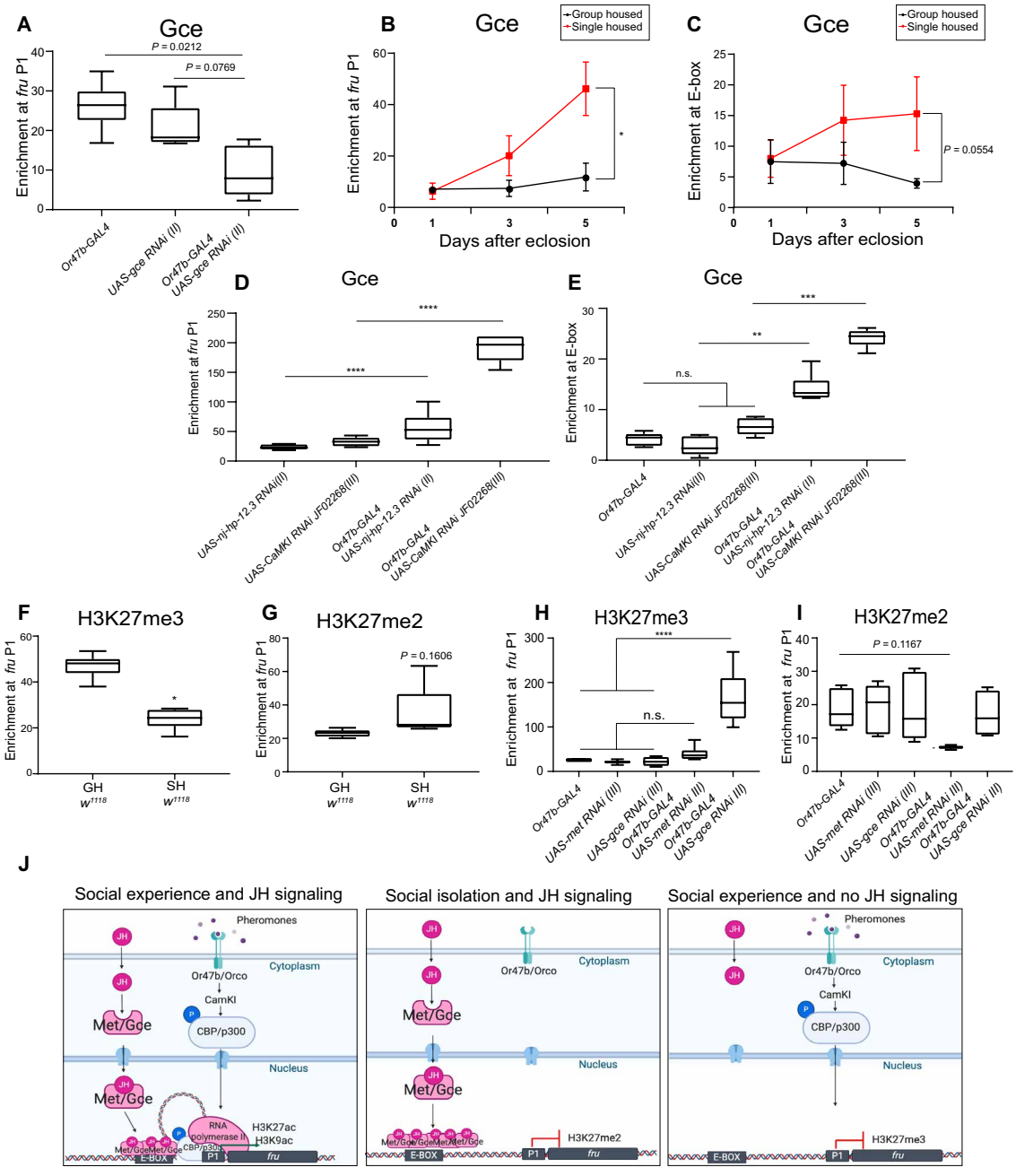

Fig. 6. JH receptor binds upstream of *fru* P1 and primes it for chromatin-based regulation with social experience. (**A**) Enrichment of Gce at *fru* P1 in 7-day-old GH male antennae with genotypes *Or47b-GAL4*, *UAS-gce RNAi*, *and Or47b-GAL4 UAS-gce RNAi*. The time course of Gce association with *fru* P1 (**B**) and E-box upstream of *fru* P1 (**C**) in GH (black) or socially isolated (red) male antennae is shown. The *x* axis shows days after eclosion, and the *y* axis is enrichment relative to input. The enrichment of Gce at *fru* P1 (**D**) or E-box (**E**) in GH male antennae with genotypes *UAS-nj(p300)RNAi*, *UAS-CaMKI RNAi*, *Or47b-GAL4 UAS-nj(p300)RNAi*, and *Or47b-GAL4 UAS-CaMKI RNAi* is shown. (**F** and **G**) Enrichment of H3K27me3 and H3K27me2 at *fru* P1 in GH or socially isolated male antennae. (**H** and **I**) Enrichment of H3K27me3 and H3K27me2 at *fru* P1 in GH male antennae with genotypes *UAS-met RNAi*, *UAS-gce RNAi*, *Or47b-GAL4 UAS-met RNAi*, *and Or47b-GAL4 UAS-gce RNAi*. (**J**) A model showing coincidence detection of hormone and pheromone signals by *fru* promoter. The presence of both social experience through pheromones and JH signaling leads to the assembly of JH receptors, activated p300, and RNA polymerase II and increases the association of active chromatin marks H3K29ac and H3K9ac at the *fru* P1. In the absence of social experience, p300 activation is inhibited, and JH receptor complexes accumulate at the *fru* P1 promoter. This leads to an increase in the association of H3K27me2, which interferes with non–cell type–specific activation of *fru* P1. In the absence of JH signaling, p300 and RNA polymerase II association decreases, and this leads to an increase in repressive chromatin marks such as H3K27me3. **P* < 0.05; ***P* < 0.005; ****P* < 0.001; *****P* < 0.0001; n.s., not significant.

The accumulation of Gce at the *fru* P1 promoter in the absence of social experience suggests that Gce complexes might function as transient repressors of transcription and that social experience converts them to transcriptional activators by stabilizing the enrichment of active chromatin marks and recruitment of basal transcriptional machinery. To test this hypothesis, we analyzed methylation state of

H3K27, where H3K27me3 is associated with repressed chromatin, whereas demethylation to H3K27me2 was shown to mark chromatin that is poised for transcription (*28*). In socially isolated males, we observed a trend toward an increase in the enrichment of poised chromatin H3K27me2 marks around *fru* P1 (Fig. 6G), compared to H3K27me3, which showed a significant decrease (Fig. 6F). Furthermore, Or47b-specific *met* and *gce RNAi* knockdowns had very little to no effect on H3K27me2, except for a small trend toward a decrease in *met* RNAi knockdowns (Fig. 6I). In contrast, H3K27me3 showed a significant increase in Or47b-specific *gce-RNAi* knockdowns. The differences between *gce* and *met* RNAi results might indicate either distinct effects for the two JH receptors in regulating the chromatin state around *fru P1* or differences in the strength of RNAi (Fig. 6, H and I).

Together, we propose a model where activity of JH receptors prime or poise fru^M transcription in ORNs, particularly Or47b neurons, which is stabilized by social experience via p300-dependent chromatin modulation around *fru* P1 (Fig. 6J). In the absence of JH signaling, fru^M is repressed and increases its association with heterochromatin marks. In contrast, in the absence of social experience, JH receptors bind to *fru* promoter and retain a poised chromatin state but cannot effectively induce *fru* expression because of lack of p300 necessary for histone acetylation and RNA polymerase II binding. Only when the two signals are coincident is *fru* expression maintained in Or47b ORNs in a stable manner. In this way, the *fru* P1 promoter act as a coincidence detector for activation at an appropriate age and social context to enhance sensory neuron responses and courtship advantage.

DISCUSSION

There is ample evidence that social experience and hormone signals are integrated by animals to modulate physiology and behavior (*2*–*4*, *23*). Interactions between hormones and social experience is vital for opening critical periods for social experience–dependent reward learning and appropriate cyclic display of mating behaviors in many organisms (*2*, *3*, *29*). Despite the known contribution of both social and hormonal cues to physiology and behaviors, molecular mechanisms regulating these changes remain unknown or poorly described. In this study, we made use of the unique advantages of the genes and circuits regulating male reproductive behaviors in *Drosophila*, which are under the control of the male-specific transcription factor Fru^M. Previous studies have shown that social experience and hormone signaling increases the sensitivity of Or47b neurons and courtship rigor in male flies (*29*–*33*). Here, we report that coincident calcium and hormone signaling converge at *fru* P1 promoter in Or47b neurons to modify chromatin and increase fru^M expression to coordinate alterations in physiology and mating behavior. Our results provide an adaptive molecular mechanism to bridge hormone and pheromone signals at the promoters of key behavioral regulators and subsequent changes in chromatin and transcription to reprogram physiology and behavior.

Chromatin modulation can provide relatively fast and possibly reversible effects on gene function in neural circuit modulation of behavior. For example, cyclic progesterone exposure, a cue indicating the ovulation state of the female mice, modulates the sensitivity of pheromone-detecting sensory neurons, which, in turn, determines whether the female will accept or will be "blind" to male courtship attempts. The change in the sensory neuron responses depend on sensory transduction components, phospholipase C–β 2 and progesterone receptor membrane component1 (PGRMC1) (*2*). It is possible that integration of social and hormone signals drives behavioral decision via chromatin-based changes in the expression of genes that dial neuronal sensitivity up or down, interfering with sensory circuit activation. Hormone signals were shown to cause changes in the chromatin landscape of actively expressed genes (*21*, *23*, *28*–*30*, *34*). Similarly, for behaviors with critical periods where sensory experience and hormone signals may be required, chromatin-based changes can also provide a way of cellular memory later in life once the chemical cues defining the critical period are gone. For example, increase in DNA methylation

Table 1. Primer list. F, forward; R, reverse.

Primer name	Sequence
ChIP qPCR primers	
FruM(−488)-ChIP F	CAGGAGCTGTTACCATTTCAC
FruM(−488)-ChIP R	CCTTTACAGTGCCCGTTTAC
FruM(+37)-ChIP F	AAATCAGCAGCCGACATAC
FruM(+37)-ChIP R	TTTACAGCGCTCTAGCATTT
FruM(+1224)-ChIP F	AGTTGGCTGAGCACAATTC
FruM(+1224)-ChIP R	ACACGGATTAGCCAGTTT
Or82a(+109)-ChIP F	GCTCTGACGTTGGCATAAC
Or82a(+109)-ChIP R	GCAGTTGAAACAGCCTACC
Gr5a(−109)-ChIP F	AATGCGACAGCTGAAAGG
Gr5a(−109)-ChIP R	TCATGGGATTCTAACGATTTGG
Or47b(+147)-ChIP F	CTTTCTGAGGTGAATCTG
Or47b(+147)-Chip R	CTTCTTGTTGGGATACTG
Kr-h1-ChIP F (+10)	CGTGACGTTCTCCGAATTT
Kr-h1-ChIP R (+135)	ACGAGATCGATTGGTAGGT
E-box-ChIP F (−7774)	GACGCATAAACGTCTTCCA
E-box-ChIP R (−7641)	CTCAGCTGCATCTCATTCTC
qRT-PCR primers	
Or47b_qPCR F	CAAATCTCAGCCTTCTGCGG
Or47b_qPCR R	GATACTGGCACAGCAAACTCA
Gal4_qPCR F	TTATGCCCAGGGATGCTCTT
Gal4_qPCR R	CGTCGCCAAAGAACCCATTA
GFP_qPCR F	ATGGAAGCGTTCAATTAGCAGA
GFP_qPCR R	AAAGGGCAGATTGTGTGGAC
fruC_qPCR F	CAAATTTGACCGGCGTGCTAACCT
fruC_qPCR R	AGTCGGAGCGGTAGTTCAGATTGT
fruM_qPCR F	CCCGCATCCCCTAGGTACAA
fruM_qPCR R	GACTGTTTCGCCCTCGCAGG
ACT5C_qPCR F	GGCGCAGAGCAAGCGTGGTA
ACT5C_qPCR R	GGGTGCCACACGCAGCTCAT
RPL13A_qPCR F	GCGAGGAGCTGAACCTCTC
RPL13A_qPCR R	GGAAGTGGAATGGACCACGG
RpLP0_qPCR F	GTGCCCATCCTGAAGCCTG
RpLP0_qPCR R	CCTGGTTGACAATCAGACCGT
TBP_qPCR F	TAAGCCCCAACTTCTCGATTCC
TBP_qPCR R	GCCAAAGAGACCTGATCCCC

patterns around glucocorticoid receptor gene with tactile maternal behaviors can have long-lasting effects on circuits and behaviors regulated by cortisol signaling (*31*–*33*, *35*). The advantage of using *Drosophila* courtship behaviors is that genes (fru^M) and circuits underlying these behaviors are well characterized. Fru^M is a male-specific transcription factor that labels the interconnected neurons in the courtship circuits and typically acts as a sexual switch during the pupal stage to alter the developmental fate of individual neurons (*6*, *7*). Fru^M can promote male fate by inhibiting cell death, altering dendritic arborization, and switching synaptic connectivity between neurons (*7*). Although Fru^M is stably expressed in the adult brain, its function in mature neurons is unknown but likely involves regulation of Fru^M downstream genes required for the function, sensitivity, and communication within and among neurons within the circuit (*36*). In this study, we uncover a previously unknown regulation of Fru^M which in turn modulates physiological properties of olfactory neurons in the adult male flies. This result is consistent with the observation that Fruitless overexpression alters the expression of several genes that are known to regulate neuronal physiology (*36*). Overall, our study shows that despite Fru^M function to masculinize the nervous system and behaviors, pheromone and hormone signals interact at *fru* P1 to regulate Fru^M expression at the level of chromatin to fine-tune neuronal properties and mating behavior. Identifying ORN-specific changes in transcription and splicing of *fru* as well as genes regulated by Fru^M in the future, combined with expanded chromatin analysis, will give insights into the genes changing neuronal sensitivity in different social conditions and age. Given the widespread interactions between hormone and sensory signals in modulating organismal behaviors, similar molecular events converging on the regulation of key behavioral genes might also modify behavioral outputs to social signals with age and reproductive state, as well as drive critical periods of social learning in vertebrates to modulate behavior (*37*–*39*).

MATERIALS AND METHODS

Fly husbandry and genetics

Flies were raised on standard fly food (containing yeast, cornmeal, agar, and molasses) at 25°C in a 12-hour light/12-hour dark cycle in cylindrical glass vials (diameter, 24 mm and height, 94 mm). For group housing, flies were collected within 12 hours of eclosion and separated by sex in groups of 15 to 30. For socially isolated flies, pupae were taken at 80 to 100 hours after pupae formation and placed into individual vials. Newly eclosed flies were transferred to fresh vials and aged until dissection. w^{1118}, *Canton S*, *Or47b* mutant alleles (*13*), $Or67d^{Gal4}/Or67d^{Gal4}$ mutant allele (*8*), and *Or47bCD2/CyO*; fru^{P1Gal4}, *40xUAS-mCD8::GFP/TM6B* were maintained at room temperature. All the flies for RNAi knockdown experiments were maintained in a 28°C incubator. These following stocks were obtained from Bloomington Stock Center: *P{TRiP.JF02097}attP2* (#26323), *Mi{MIC}gceMI02742* (#60189), *P{TRiP.HMJ23341}attP40* (#61852), Met^1 (#3472), *P{TRiP.JF02103}attP2* (#26205), *P{TRiP.HMJ23518}attP40* (#61935), *P{UAS-nej.siRNA}hp12* (#32576), *P{UAS-nej.siRNA}hp12.3* (#32579), *P{TRiP.JF02268}attP2* (#26726), *P{TRiP.GL00274}attP2* (#35362), and *Or47b-GAL4*. For temperature shift experiments to define the critical period of JH receptor function, we raised *UAS-gce RNAi* and *UAS-met RNAi* crosses at 28°C. The progeny was transferred to 22°C to decrease RNAi knockdown at eclosion, day 2, and day 3, and fru^{P1GAL4}-driven GFP expression is analyzed at day 7.

Genotypes

Figure 1

Figure 1A. w^{1118}

Figure 1B. *Canton S and* w^{1118}

Figure 1C. w^{1118}, $Or47b^1/Or47b^1$; *TM2/TM6B*, $Or47b^2/Or47b^2$; *TM2/TM6B*; $Or67d^{Gal4}/Or67d^{Gal4}$

Figure 1 (D to G). w^{1118}

Figure 2

Figure 2 (A to C). *Or47b-CD2/CyO*; fru^{P1Gal4}, *40xUAS-mCD8::GFP/TM6B*

Figure 2D. w^{1118}

Figure 3

Figure 3 (A to F). *Or47b-CD2/CyO*; fru^{P1Gal4}, *40xUAS-mCD8::GFP/TM6B*

Figure 3 (G and H). w^{1118}

Figure 4

Or47b-Gal4 UAS-mCD8::GFP/CyO; TM2/TM6B

UAS-nej hp12 RNAi(X)/+

UAS-nej hp12.3 RNAi(II)/CyO

UAS-CamKI GL01332 RNAi(III)/TM6B

UAS-CamKI JF02268 RNAi(III)/TM6B

UAS-nej hp12 RNAi(X)/+; Or47b-Gal4 UAS-mCD8::GFP/CyO; TM2/TM6B

UAS-nej hp12.3 RNAi(II)/Or47b-Gal4 UAS-mCD8::GFP; TM2/TM6B

Or47b-Gal4 UAS-mCD8::GFP/CyO; UAS-CamKI GL01332 RNAi(III)/TM6B

Or47b-Gal4 *UAS-mCD8::GFP/CyO; UAS-CamKI JF02268 RNAi(III)/TM6B*

Figure 5

Figure 5 (A, B, D to F)

Or47b-CD2/CyO; fru^{P1Gal4}, *40xUAS-mCD8::GFP/TM6B*

Or47b-CD2/UAS-gce HMJ23341 RNAi(II); fru^{P1Gal4}, *40xUAS-mCD8::GFP/TM6B*

Or47b-CD2/CyO; fru P1Gal4, *40xUAS-mCD8::GFP/UAS-gce JF02097 RNAi(III)*

met^1/+; *Or47b-CD2/CyO; fru P1Gal4*, *40xUAS-mCD8::GFP/TM6B*

Or47b-CD2/CyO; fru^{P1Gal4}, *40xUAS-mCD8::GFP/UAS-met JF02103 RNAi(III)*

Or47b-CD2/UAS-met HMJ23518 RNAi(II); fru^{P1Gal4}, *40xUAS-mCD8::GFP/TM6B*

Figure 5C

UAS-met HMJ23518 RNAi(II)/CyO; TM2/TM6B

UAS-gce HMJ23341 RNAi(II)/CyO; TM2/TM6B

Or47b-Gal4, *UAS-mCD8::GFP/UAS-met HMJ23518 RNAi(II); TM2/TM6B*

Or47b-Gal4, *UAS-mCD8::GFP/UAS-gce HMJ23341 RNAi(II); TM2/TM6B*

Figure 6

Figure 6A

Or47b-Gal4 UAS-mCD8::GFP/CyO; TM2/TM6B

UAS-gce HMJ23341 RNAi(II)/CyO; TM2/TM6B

Or47b-Gal4, *UAS-mCD8::GFP/UAS-gce HMJ23341 RNAi(II); TM2/TM6B*

Figure 6 (B, C, F, and G). w^{1118}

Figure 6 (D and E)

UAS-nej hp12.3 RNAi(II)/CyO

UAS-CamKI JF02268 RNAi(III)/TM6B

UAS-nej hp12.3 RNAi(II)/Or47b-Gal4, *UAS-mCD8::GFP; TM2/TM6B*

Or47b-Gal4, *UAS-mCD8::GFP/CyO; UAS-CamKI JF02268 RNAi(III)/TM6B*
Or47b-Gal4 UAS-mCD8::GFP/CyO; TM2/TM6B
Figure 6 (H and I)
Or47b-Gal4 UAS-mCD8::GFP/CyO; TM2/TM6B
UAS-met JF02103 RNAi(III)
UAS-gce JF02097 RNAi(III)/TM6B
Or47b-Gal4, UAS-mCD8::GFP/CyO; UAS-met JF02103 RNAi(III)/TM6B
Or47b-Gal4, UAS-mCD8::GFP/CyO; UAS-gce JF02097 RNAi(III)/TM6B

Figure S1
Figure S1 (A to F). w^{1118}
Figure S1 (G to M). *Or47b-CD2/CyO*; fru^{P1Gal4}, *40xUAS-mCD8::GFP/TM6B*

Figure S2
Figure S2 (A to F)
Or47b-Gal4, UAS-mCD8::GFP/CyO; TM2/TM6B
UAS-nej hp12 RNAi(X)/+
UAS-nej hp12.3 RNAi(II)/CyO
UAS-CamKI GL01332 RNAi(III)/TM6B
UAS-CamKI JF02268 RNAi(III)/TM6B
UAS-nej hp12 RNAi(X)/+; Or47b-Gal4, UAS-mCD8::GFP/CyO; TM2/TM6B
Or47b-Gal4, UAS-mCD8::GFP/UAS-nej hp12.3 RNAi(II); TM2/TM6B
Or47b-Gal4, UAS-mCD8::GFP/CyO; UAS-CamKI GL01332 RNAi(III)/TM6B
Or47b-Gal4, *UAS-mCD8::GFP/CyO; UAS-CamKI JF02268 RNAi(III)/TM6B*

Figure S3
Or47b-Gal4, UAS-mCD8::GFP/CyO; TM2/TM6B
UAS-nej hp12.3 RNAi(II)/CyO
UAS-CamKI JF02268 RNAi(III)/TM6B
Or47b-Gal4, UAS-mCD8::GFP/UAS-nej hp12.3 RNAi(II)
Or47b-Gal4, *UAS-mCD8::GFP/CyO; UAS-CamKI JF02268 RNAi(III)/TM6B*

Figure S4
UAS-met HMJ23518 RNAi(II)/CyO; TM2/TM6B
UAS-gce HMJ23341 RNAi(II)/CyO; TM2/TM6B
Or47b-Gal4, UAS-mCD8::GFP/UAS-met HMJ23518 RNAi(II); TM2/TM6B
Or47b-Gal4, UAS-mCD8::GFP/UAS-gce HMJ23341 RNAi(II); TM2/TM6B

Social condition

For social isolation condition, males were isolated into separate vials as pharate adults in pupal case, allowed to eclose alone, and aged as SH to different ages to deprive pheromone input from Or47b ORNs. For GH condition, 15 to 30 newly eclosed males were collected and aged as GH until dissection. Dissections were performed at 1, 2, 3, 5, 7, 9, 10, and 11 days, dependent on experiment. For rescue experiments in the absence of PA exposure, SH flies were regrouped at days 1, 3, and 5 in group of 35 flies and taken out to combinations of days 5, 7, 9, and 11 to examine the effect of duration of social experience on the epigenetic modification around fru^{P1} promoter.

Odor and pharmacological treatment

To examine the effect of PA on *fru* expression in socially isolated flies, 0.45 mg of PA (Cayman) or 10 μl of ethanol (solvent control) (E7023, Sigma-Aldrich) was applied on a piece of filter paper (1 cm by 1 cm) and air-dried in the hood for 60 min. The filter paper containing PA or solvent control was then transferred to a fresh vial with an SH fly. Fresh filter paper was changed every other day.

Immunohistochemistry

Flies from the *Or47b-CD2/CyO*; fru^{P1Gal4}, *40xUAS-mCD8::GFP/TM6B* stock were used for fru^{M} expression quantification. Fly heads were removed in PBT (phosphate buffered saline with Triton X) and fixed in 4% paraformaldehyde (PFA) for 1 hour, followed by three 15-min PBT washes. Antennae were removed from the head in PBT and fixed in 4% PFA for 0.5 hours, followed by three 15-min PBT washes. Antennae were incubated in primary antibody 1:200 mouse mouse-α-Rat-CD2 (Bio-Rad, MCA154GA) and 5% normal goat serum (NGS) at 4°C overnight, followed by three 15-min PBT washes, and then incubated in secondary antibody 1:1000 goat α-mouse-Cy3 and 5% NGS at 4°C overnight. Antennae were mounted using Fluoromount-G mounting solution (SouthernBiotech) and imaged. Confocal images were taken using the following confocal microscopes: Olympus FluoView FV1000 with laser power 488 = 17%, intensity = 710, pinhole = 105 μm, gain = 1, and offset = −1; Zeiss 510 with argon laser power = 35%, pinhole = 108 μm, detector gain = 800, amplifier gain = 1, and amplifier offset = −0.185.

Fluorescence quantification

fru^{P1GAL4}-driven *UAS-GFP* expression was quantified using ImageJ. Individual Or47b or Or67d ORN cell body boundaries were drawn and kept identical for each cell body. Integrated fluorescence density (for images taken using Zeiss 510) and fluorescence intensity (for images taken using Olympus FluoView FV1000) of the cell boundary for each ORN were measured using ImageJ fluorescence analysis tools. Or47b ORN cell bodies were identified on the basis of the presence of *Or47b-CD2* marker. Or67d ORN cell bodies were identified on the basis of the absence of *Or47b-CD2* marker and their central location on the antennae. Fifteen to 25 images per experimental condition were quantified, and statistical tests were performed in GraphPad Prism.

Chromatin immunoprecipitation and qPCR

ChIP protocol was modified from (*38*, *39*). For each genotype, roughly 180 third antennal segments were cross-linked in 1.22% formaldehyde in dissection buffer for 10 min at 1 μl per antennae. Samples were quenched with 2.5 M glycine to a final concentration of 125 nM. Antennae were ground via electric mortar and biorupted in the Eppendorf Bioruptor for 30 cycles at 30-s on/off cycles. See (*39*) for post-bioruption protocol using the following antibodies: H3K27ac (ab4729), H3K9ac (ab4441), and RNA polymerase II (Millipore, 05-623), H3K27me2 (ab24684), and H3K27me3 (ab6002), while control sample tubes contain no antibody. P300 and GCE antibodies were gifts from M. Mannervik (*40*) and C. Desplan, respectively. For primer pairs and reagents for qPCR DNA amplification against *fru* P1, see the "Quantitative RT-PCR" section below. To ensure that any differences in *fru* P1 enrichments were site specific, we examined Or82a, Or47b, and Gr5a promoters; all primers can be found in Table 1 below. Data were processed using a modified $2^{-\Delta Ct}$ calculations to determine the percent enrichment. We define fold enrichment as $(1 + \text{amplification efficiency})^{(-((\text{Ct antibody}) - (\text{CtnoAntibody})))}$, where amplification efficiency is calculated from the standard curve of the primer pair.

Quantitative RT-PCR

Antennae from 100 male flies were dissected on CO_2 pads and transferred into TRIzol (Ambion Life Technologies). At least three biological replicates were prepared for each genotype. RNA was extracted using the RNeasy kit (QIAGEN) and reverse-transcribed using the SuperScript IV First-Strand Synthesis Kit (Invitrogen). qPCR was performed using the FastStart Universal SYBR Green Master (ROX) kit (Roche) on Eppendorf Realplex. Primers used were listed in Table 1. The expression level of each gene was normalized to the expression of actin, and the relative expression level was compared across experimental conditions using the delta-delta Ct method. Statistical tests were performed in GraphPad Prism.

Statistical analysis

Fifteen to 25 antennae were used for GFP quantifications in different social and mutant conditions. For fluorescence analysis, one-way analysis of variance (ANOVA) followed by Bonferroni's multiple comparisons tests was performed to assess statistical significance between conditions. For each ChIP experiment, we used two to three biological replicates (n), which are derived from a pool of 180 third antennal segments per biological replicate. For each of the biological replicates, we performed three technical replicates of the ChIP-qPCR. Across sample preparations, fold enrichment was standardized to the wild-type sample values within each experiment, i.e., wild-type GH sample fold enrichment values were used to normalize across different biological preparations to control for batch effects. In addition, no-antibody Ct values were standardized within a plate to limit well effects. To assess significance of the effects of genotype, we then used a nested ANOVA, followed by post hoc comparisons among genotypes and treatments, using the two-stage step-up method of Benjamini, Keieger, and Yekutieli in GraphPad Prism to correct for multiple testing by controlling the false discovery rate. For qRT-PCR experiments, we performed three to four biological replicates, each from a pool of 100 to 200 antennae. To assess effects of social condition, we used two-tailed t test. For ChIP, $P > 0.2$ (not significant), and P value between 0.05 and 0.2 provide the numerical value (all: *$P < 0.05$, **$P < 0.005$, ***$P < 0.001$, and ****$P < 0.0001$).

Figure 1

Figure 1A. For time course experiments, we ran a nested t test on GH versus SH time points as whole.

Pol II GH w^{1118} compared by day: SH w^{1118} 180 whole antennae ($P = 0.0031$, $n = 8$)

H3K27ac GH w^{1118} compared by day: SH w^{1118} 180 whole antennae ($P < 0.0001$, $n = 8$)

Figure 1B. GH w^{1118}: SH w^{1118} 180 whole antennae ($P = 0.0338$, $n = 3$), GH *Canton S* 180 whole antennae ($P = 0.8475$., $n = 2$), SH *Canton S* ($P = 0.0560$, $n = 2$).

Figure C. GH w^{1118}: SH w^{1118} 180 whole antennae ($P = 0.0391$, $n = 3$), $Or47b^{1/1}$ ($P = 0.0246$, $n = 3$), $Or47b^{2/2}$($P = 0.1120$, $n = 2$), $Or67d^{GAL4}/Or67d^{GAL4}$ ($P = 0.7828$, $n = 2$), $Or47b^{1/1}$: SH w^{1118} 180 whole antennae ($P = 0.7828$, $n = 3$), $Or47b^{2/2}$($P = 0.2617$, $n = 2$), $Or67d^{GAL4}/Or67d^{GAL4}$ ($P = 0.0179$, $n = 2$).

Figure 1C′. SH w^{1118} 180 whole antennae ($P = 0.0007$, $n = 3$), $Or47b^{1/1}$ ($P = 0.0008$, $n = 2$).

Figure 1C″. SH w^{1118} 180 whole antennae ($P = 0.0306$, $n = 2$), $Or47b^{1/1}$ ($P = 0.0295$, $n = 2$), $Or47b^{2/2}$ ($P = 0.0445$, $n = 2$), $Or67d^{GAL4}/Or67d^{GAL4}$ ($P = 0.0002$, $n = 2$).

Figure 1C‴. SH w^{1118} 180 whole antennae ($P = 0.0360$, $n = 2$), $Or47b^{1/1}$ ($P = 0.0342$, $n = 2$), $Or67d^{GAL4}/Or67d^{GAL4}$ ($P = 0.0002$, $n = 2$).

Figure 1D. RNA PolII; *Or47b*: GH versus SH w^{1118} ($P = 0.6365$, $n = 2$); *Or82a*: GH versus SH w^{1118} ($P = 0.5283$, $n = 2$); *Gr5a*: GH versus SH w^{1118} ($P = 0.8865$, $n = 2$).

Figure 1E. p300; *Or47b*: GH versus SH w^{1118} ($P = 0.5192$, $n = 2$); *Or82a*: GH versus SH w^{1118} ($P = 0.7744$, $n = 2$); *Gr5a*: GH versus SH w^{1118} ($P = 0.3698$, $n = 2$).

Figure 1F. H3K9ac; *Or47b*: GH versus SH w^{1118} ($P = 0.4366$, $n = 2$); *Or82a*: GH versus SH w^{1118} ($P = 0.1420$, $n = 2$); *Gr5a*: GH versus SH w^{1118} ($P = 0.7075$, $n = 2$).

Figure 1G. H3K27ac; *Or47b*: GH versus SH w^{1118} ($P = 0.4816$, $n = 2$); *Or82a*: GH versus SH w^{1118} ($P = 0.0899$, $n = 2$); *Gr5a*: GH versus SH w^{1118} ($P = 0.7918$, $n = 2$).

Figure 2

Figure 2 (B and C). Two-way ANOVA followed by Bonferroni's multiple comparisons test.

In Or47b neurons, fru^{P1GFP} expression is significantly higher in flies raised in group housing condition compared to social isolation in 2-day-old ($P < 0.0001$, $n = 1182$ for SH, $n = 530$ for GH), 5-day-old ($P = 0.0025$, $n = 1229$ for SH, $n = 1665$ for GH), and 7-day-old ($P < 0.0001$, $n = 1602$ for SH, $n = 1516$ for GH) males. In Or67d neurons, fru^{P1GFP} expression is unaffected by social experience in 5-day-old ($P = 0.8511$, $n = 1115$ for SH, $n = 1430$ for GH) and 7-day-old ($P > 0.9999$, $n = 1285$ for SH, $n = 1133$ for GH) males. However, fru^{P1GFP} expression is significantly higher in socially isolated flies in 2-day-old male compared to flies raised in group housing condition ($P = 0.0054$, $n = 1015$ for SH, $n = 374$ for GH).

Figure 2D. Two-tailed t test.

fru^{M} expression is significantly higher in GH males at day 5 ($P = 0.016$, $t = 3.321$, $df = 6$) and day 7 ($P = 0.01$, $t = 3.709$, $df = 6$). However, fru^{M} expression is significantly higher in socially isolated males at day 2 ($P = 0.0126$, $t = 3.514$, $df = 6$).

fru^{C} expression remains unchanged by social condition in 2-day-old males ($P = 0.6901$, $t = 0.4185$, $df = 6$) and 7-day-old-males ($P = 0.2203$, $t = 1.368$, $df = 6$). fru^{C} expression is significantly higher in socially isolated males at day 5 ($P = 0.0341$, $t = 2.733$, $df = 6$).

Figure 3

Figure 3 (B to F). One-way ANOVA followed by Bonferroni's multiple comparisons test.

Figure 3B. Compared to 5d SH + solvent, there is significantly higher fru^{P1GFP} expression in Or47b neurons in 5d GH + solvent flies ($P < 0.0001$, $n = 1054$). Applying PA at eclosion leads to significant increase in fru^{P1GFP} expression ($P < 0.0001$, $n = 1218$), rescuing fru^{P1GFP} expression toward the GH level ($P < 0.0001$, $n = 1054$), whereas applying PA at day 3 leads to significant decrease in fru^{P1GFP} expression ($P < 0.0001$, $n = 427$).

Figure 3C. In Or67d neurons, the fru^{P1GFP} expression is unaffected by social experience ($P = 0.5152$, $n = 540$), application of PA at eclosion ($P > 0.9999$, $n = 769$), or at day 3 ($P > 0.9999$, $n = 414$), compared to 5d SH + solvent.

Figure 3E. In Or47b neurons, applying PA at day 2 ($P < 0.0001$, $n = 624$) or day 3 ($P < 0.0001$, $n = 779$) both led to significant increase in fru^{P1GFP} expression level in flies lacking social experience, bringing the level to GH level when applied at day 2 ($P > 0.9999$, $n = 428$) and day 3 ($P = 0.2221$, $n = 478$).

Figure 3F. In Or67d neurons, applying PA at day 2 ($P = 0.2973$, $n = 505$) does not result in difference in fru^{P1GFP} expression compared to in flies raised in social isolation. However, applying PA at day 3 leads to significant increase in fru^{P1GFP} expression compared to both SH ($P < 0.0001$, $n = 677$) and GH flies ($P < 0.0001$, $n = 737$) applied with solvent controls.

Figure 3 (G to I). All ChIP were analyzed with ANOVA followed by post hoc multiple comparison.

Figure 3G. GH w^{1118}: Regroup 1d > 5d (P = 0.0701, n = 2), Regroup 3d > 5d (P = 0.0036, n = 2), Regroup 3d > 7d (P = 0.1041, n = 2), Regroup 5d > 9d (P = 0.0100,n = 2), SH w^{1118} 5d (P = 00384, n = 2); Regroup 1 > 5d: Regroup 3d > 5d (P = 0.1116, n = 2), Regroup 3d > 7d (P = 0.6642, n = 2), Regroup 5d > 9d (P = 0.2397, n = 2), SH w^{1118} 5d (P = 0.1335, n = 2); Regroup 3d > 7d: Regroup 5d > 9d (P = 0.1032, n = 2), SH w^{1118} 5d (P = 0.0526, n = 2); Regroup 5d > 9d: SH w^{1118} 5d (P = 0.7010, n = 2).

Figure 3H. 7 day GH w^{1118}: Regroup 1d > 7d (P = 0.6423, n = 2), Regroup 3d > 9d (P = 0.0827, n = 2), Regroup 5d > 11d (P = 0.9142, n = 2), SH w^{1118} 7d (P = 0.0014, n = 2); Regroup 1 > 7d: Regroup 3d > 9d (P = 0.0350, n = 2), Regroup 5d > 11d (P = 0.6743, n = 2), SH w^{1118} 7d (P = 0.0007, n = 2); Regroup 3d > 9d: Regroup 5d > 11d (P = 0.0446, n = 2), SH w^{1118} 7d (P = 0.0080, n = 2); Regroup 5d > 11d; SH w^{1118} 7d (P = 0.0006, n = 2).

Figure 3I. GH w^{1118}: Regroup 1d > 5d (P = 0.1587, n = 2), Regroup 3d > 5d (P = 0.2342, n = 2), SH w^{1118} 5d (P = 0.0109, n = 2); Regroup 1d > 5d: Regroup 3d > 5d (P = 0.0109, n = 2), SH w^{1118} 5d (P = 0.0125, n = 2).

Figure 4

All ChIP analyzed with nested ANOVA followed by post hoc multiple comparison controlling for false discovery.

Figure 4A. All component comparisons (P > 0.05); *Or47b-GAL4: Or47b-GAL4 UAS-nj-hp 12 RNAi(X)* (P = 0.0013, n = 2) *Or47b-GAL4 UAS-nj-hp 12.3(II)* (P = 0.0020, n = 2), *O47b-GAL4 UAS-CamKI RNAi GL01332 (III)* (P = 0.0011, n = 2), *Or47b-GAL4 UAS-CamKI RNAi JF02268 (III)* (P = 0.0014, n = 2).

Figure 4B. *Or47b-GAL4: Or47b-GAL4 UAS-nj-hp 12 RNAi(X)* (P = 0.0002, n = 2) *Or47b-GAL4 UAS-nj-hp 12.3(II)* (P < 0.0001, n = 2), *O47b-GAL4 UAS-CamKI RNAi GL01332 (III)* (P < 0.0001, n = 2), *Or47b-GAL4 UAS-CamKI RNAi JF02268 (III)* (P < 0.0001, n = 2).

Figure 4C. All component comparisons (P > 0.05); *Or47b-GAL4: Or47b-GAL4 UAS-nj-hp 12 RNAi(X)* (P = 0.0075, n = 2), *Or47b-GAL4 UAS-CamKI RNAi JF02268 (III)* (P = 0.0046, n = 2).

Figure 4D. All component comparisons (P > 0.05) except *UAS-CamKI RNAi GL01332 (III)* (P = 0.0120, n = 2); *Or47b-GAL4: Or47b-GAL4 UAS-nj-hp 12 RNAi(X)* (P < 0.0001, n = 2) *Or47b-GAL4 UAS-nj-hp 12.3(II)* (P = 0.0001, n = 2), *O47b-GAL4 UAS-CamKI RNAi GL01332 (III)* (P < 0.0001, n = 2), *Or47b-GAL4 UAS-CamKI RNAi JF02268 (III)* (P < 0.0001, n = 2).

Figure 5

Figure 5B. All genotypes were analyzed with one-way ANOVA followed by Bonferroni's multiple comparisons test.

Comparing to fru^{P1Gal4}, fru^{P1Gal4} *UAS-gce RNAi (III)* Or47b neurons (P < 0.0001, n = 513), Or67d neurons (P < 0.0001, n = 388)

fru^{P1Gal4} *UAS-gce RNAi (II)* Or47b neurons (P = 0.0203, n = 532), Or67d neurons (P < 0.0001, n = 534)

fru^{P1Gal4} *UAS-met RNAi (II)* Or47b neurons (P < 0.0001, n = 542), Or67d neurons (P > 0.9999, n = 616)

met^{1}; fru^{P1Gal4} Or47b neurons (P < 0.0001, n = 492), Or67d neurons (P = 0.0013, n = 460)

fru^{P1Gal4} *UAS-met RNAi (III)* Or47b neurons (P < 0.0001, n = 680), Or67d neurons (P = 0.0029, n = 617).

Figure 5C. RNA polymerase II. *Or47b-GAL4: Or47b-GAL4 UAS-met RNAi (II)* (P = 0.0018, n = 2), *Or47b-GAL4 UAS-gce RNAi (II)* (P = 0.0044, n = 2); *UAS-met RNAi (II): Or47b-GAL4 UAS-met RNAi (II)* (P = 0.0074, n = 2), *UAS-gce RNAi (II): Or47b-GAL4 UAS-gce RNAi (II)* (P = 0.2249, n = 2)

p300. *Or47b-GAL4: Or47b-GAL4 UAS-met RNAi (II)* (P = 0.0581, n = 2), *Or47b-GAL4 UAS-gce RNAi (II)* (P = 0.0425, n = 2); *UAS-met RNAi (II): Or47b-GAL4 UAS-met RNAi (II)* (P = 0.0116, n = 2), *UAS-gce RNAi (II): Or47b-GAL4 UAS-gce RNAi (II)* (P = 0.0081, n = 2)

H3K27ac. *Or47b-GAL4: Or47b-GAL4 UAS-met RNAi (II)* (P = 0.0024, n = 2), *Or47b-GAL4 UAS-gce RNAi (II)* (P = 0.0095, n = 2); *UAS-met RNAi (II): Or47b-GAL4 UAS-met RNAi (II)* (P = 0.0012, n = 2), *UAS-gce RNAi (II): Or47b-GAL4 UAS-gce RNAi (II)* (P = 0.0421, n = 2).

Figure 5 (D and E). All genotypes were analyzed with two-way ANOVA followed by Bonferroni's multiple comparisons test.

Comparing to WT 28°C → 22°C eclosion, *met RNAi* → 22°C eclosion Or47b neurons (P < 0.0001, n = 1323), Or67d neurons (P < 0.0001, n = 1394); *gce RNAi* → 22°C eclosion Or47b neurons (P < 0.0001, n = 535), Or67d neurons (P < 0.0001, n = 762).

Comparing to WT 28°C → 22°C day 2, *met RNAi* → 22°C day 2 Or47b neurons (P = 0.9753, n = 1449), Or67d neurons (P < 0.0001, n = 1252).

gce RNAi → 22°C day 2 Or47b neurons (P < 0.0001, n = 796), Or67d neurons (P < 0.0001, n = 1021).

Comparing to WT 28°C → 22°C day 3, *met RNAi* →22°C day 3 Or47b neurons (P < 0.0264, n = 441), Or67d neurons (P < 0.0001, n = 543); *gce RNAi* → 22°C day 3 Or47b neurons (P > 0.9999, n = 600), Or67d neurons (P < 0.0001, n = 761).

Comparing to WT at 28°C, *met RNAi* at 28°C Or47b neurons (P < 0.0001, n = 1342), Or67d neurons (P < 0.0001, n = 999); *gce RNAi* 28°C Or47b neurons (P < 0.0001, n = 443), Or67d neurons (P < 0.0001, n = 454).

Figure 6

All ChIP data were analyzed with nested ANOVA followed by post hoc multiple comparison controlling for false discovery.

Figure 6A. *Or47b-GAL: Or47b-GAL4 UAS-gce RNAi (III)* (P = 0.0212, n = 2); *UAS-gce RNAi (III): Or47b-GAL4 UAS-gce RNAi (III)* (P = 0.0769, n = 2).

For time course experiments, we ran a nested *t* test on GH versus SH time points as whole.

Figure 6B. GH w^{1118} comparison: SH w^{1118} 180 whole antennae (P = 0.0345, n = 6).

Figure 6C. GH w^{1118} comparison: SH w^{1118} 180 whole antennae (P = 0.0554, n = 6); all experimental comparisons (P < 0.0001, n = 2); all control comparisons (P > 0.05, n = 2).

Figure 6E. *Or47b-GAL4: Or47b-GAL4 UAS-nj-hp 12.3 RNAi (II)* (P = 0.0013, n = 2): *Or47b-GAL4 UAS-CamKI RNAi JF02268 (II)* (P < 0.0001, n = 2); *UAS-nj-hp 12.3 RNAi (II): Or47b-GAL4 UAS-nj-hp 12.3 RNAi (II)* (P = 0.0007, n = 2); *UAS-CamKI RNAi JF02268 (II): Or47b-GAL4 UAS-CamKI RNAi JF02268 (II)* (P < 0.0001, n = 2).

Figure 6F. H3K27me3 GH versus SH w^{1118} (P = 0.0226, n = 2).

Figure 6G. H3K27me2 GH versus SH w^{1118} (P = 0.1606, n = 2).

Figure 6H. H3K27me2; *Or47b-GAL: Or47b-GAL4 UAS-met RNAi (III)* (P = 0.1167, n = 2), *Or47b-GAL4 UAS-gce RNAi (III)* (P = 0.8249, n = 2);*UAS-met RNAi (III): Or47b-GAL4 UAS-met RNAi (III)* (P = 0.4058, n = 2); *Or47b-GAL4 UAS-gce RNAi (III)* (P < 0.4901., n = 2); *UAS-gce RNAi (III): Or47b-GAL4 UAS-met RNAi (III)* (P = 0.1834, n = 2); *Or47b-GAL4 UAS-gce RNAi (III)* (P < 0.9243, n = 2).

Figure 6I. H3K27me3; *Or47b-GAL: Or47b-GAL4 UAS-met RNAi (III)* (P = 0.3066, n = 2), *Or47b-GAL4 UAS-gce RNAi (III)* (P < 0.0001, n = 2); *UAS-met RNAi (III): Or47b-GAL4 UAS-met RNAi (III)* (P = 0.2842, n = 2); *Or47b-GAL4 UAS-gce RNAi (III)*

($P < 0.0001$, $n = 2$); *UAS-gce RNAi (III): Or47b-GAL4 UAS-met RNAi (III)* ($P = 0.31363578$, $n = 2$); *Or47b-GAL4 UAS-gce RNAi (III)* ($P < 0.0001$, $n = 2$).

Figure S1

Whole antennal gene expressions in different social conditions were analyzed by two-tailed *t* tests.

Figure S1A. *Or47b* expression remains unaffected by social condition in 2-day-old ($P = 0.5896$, $t = 0.5697$, $df = 6$), 5-day-old ($P = 0.5281$, $t = 0.6695$, $df = 6$), and 7-day-old ($P = 0.2427$, $t = 1.296$, $df = 6$) males.

Figure S1B. *Or13a* expression remains unaffected by social condition in 2 day ($P = 0.9764$, $t = 0.03086$, $df = 6$), 5-day-old ($P = 0.1943$, $t = 1.461$, $df = 6$), and 7-day-old Wt males ($P = 0.3049$, $t = 1.122$, $df = 6$).

Figure S1C. *Or22a* expression remains unaffected by social condition in 2 day ($P = 0.8246$, $t = 0.2315$, $df = 6$) and 7 day ($P = 0.8325$, $t = 0.2209$, $df = 6$); *or22a* expression is significantly higher in GH flies at day 5 ($P = 0.0021$, $t = 5.161$, $df = 6$).

Figure S1D. *Or65a* expression remains unaffected by social condition in 2 day ($P = 0.709$, $t = 0.3915$, $df = 6$), 5 day ($P = 0.8744$, $t = 0.1664$, $df = 5$), and 7 day ($P = 0.6231$, $t = 0.178$, $df = 6$).

Figure S1E. Ribosomal protein average *(rplp0* and *rpl13a)* expression remains unaffected by social condition in 2 day ($P = 0.986$, $t = 0.01824$, $df = 6$) and 7 day ($P = 0.986$, $t = 0.01824$, $df = 6$). Ribosomal protein average expression is significantly higher in GH flies at day 5 ($P = 0.0194$, $t = 3.392$, $df = 5$).

Figure S1F. *tbp* expression remains unaffected by social condition in 2 day ($P = 0.8051$, $t = 0.2578$, $df = 6$), 5 day ($P = 0.329$, $t = 1.062$, $df = 6$), and 7 day ($P = 0.61$, $t = 0.5379$, $df = 6$).

Figure S1G. fru^M expression is significantly higher in GH males in 5-day-old ($P = 0.012$, $t = 3.497$, $df = 6$) and 7-day-old ($P = 0.045$, $t = 2.515$, $df = 6$) *Wt* males.

Figure S1H. fru^C expression remains unchanged by social condition in 7d *Wt* male ($P = 0.9303$, $t = 0.091$, $df = 6$). fru^C expression is significantly higher in socially isolated males in 5-day-old ($P = 0.017$, $t = 1.733$, $df = 6$) *Wt* male.

Figure S1I. *gal4* expression is significantly higher in GH males in 5-day-old ($P = 0.0039$, $t = 4.56$, $df = 6$) and 7-day-old ($P = 0.031$, $t = 2.118$, $df = 6$) *Wt* males.

Figure S1J. *gfp* expression is higher in GH males in 5-day-old ($P = 0.0564$, $t = 2.66$, $df = 4$) and 7-day-old ($P = 0.0025$, $t = 4.983$, $df = 6$) *Wt* males.

Figure S1K. *Or47b* expression remains unaffected by social condition in 5-day-old ($P = 0.4444$, $t = 0.8184$, $df = 6$) and 7-day-old ($P = 0.556$, $t = 0.6233$, $df = 6$) *Wt* males.

Figure S1L. Ribosomal protein average *(rplp0* and *rpl13a)* expression remains unaffected by social condition in 5-day-old ($P = 0.81$, $t = 0.2534$, $df = 5$) and 7-day-old ($P = 0.2386$, $t = 1.308$, $df = 6$) *Wt* males.

Figure S1M. *tbp* expression remains unaffected by social condition in 5-day-old ($P = 0.2666$, $t = 1.225$, $df = 6$) and 7-day-old ($P = 0.2722$, $t = 1.209$, $df = 6$) *Wt* males.

Figure S2

Figure S2A. All comparison $P > 0.05$ and $n = 2$ per condition.

Figure S2B. Comparisons with ($P < 0.05$), *UAS-nj-hp 12.3 RNAi (II): Or47b-GAL4 UAS-nj-hp 12 RNAi(X)* ($P = 0.0167$, $n = 2$), *Or47b-GAL4 UAS-nj-hp 12.3(II)* ($P = 0.0150$, $n = 2$), *O47b-GAL4 UAS-CamKI RNAi GL01332 (III) (P = 0.0179, n = 2)*, *Or47b-GAL4 UAS-CamKI RNAi JF02268 (III)* ($P = 0.0182$, $n = 2$).

Figure S2C. All comparisons $P > 0.05$ and $n = 2$ per condition.

Figure S2D. All comparisons $P > 0.05$ and $n = 2$ per condition.

Figure S2E. Comparisons with $P < 0.05$: *Or47b-GAL4, UAS-nj-hp 12.3 RNAi (II),and UAS-nj-hp 12 RNAi(X)* versus *Or47b-GAL4 UAS-CamKI RNAi JF02268 (III)*, *O47b-GAL4 UAS-CamKI RNAi GL01332 (III)*, *Or47b-GAL4 UAS-nj-hp 12 RNAi(X)*, *Or47b-GAL4 UAS-nj-hp 12.3(II)*.

Figure S2F. All comparisons $P > 0.05$ and $n = 2$ per condition

Figure S3

Figure S3A. *Or47b-GAL4*: *UAS-nj-hp 12.3 RNAi (II)* ($P = 0.4535$, $n = 2$), *UAS-CamKI RNAi JF02268 (II)* ($P = 0.1591$, $n = 2$), *Or47b-GAL4 UAS-nj-hp 12.3 RNAi (II)* ($P = 0.9570$, $n = 2$): *Or47b-GAL4 UAS-CamKI RNAi JF02268 (II)* ($P = 0.1107$, $n = 2$); *UAS-nj-hp 12.3 RNAi (II): Or47b-GAL4 UAS-nj-hp 12.3 RNAi (II)* ($P = 0.9570$, $n = 2$); *UAS-CamKI RNAi JF02268 (II): Or47b-GAL4 UAS-CamKI RNAi JF02268 (II)* ($P < 0.4840$, $n = 2$).

Figure S3B. *Or47b-GAL4*: *UAS-nj-hp 12.3 RNAi (II)* ($P = 0.6996$, $n = 2$), *UAS-CamKI RNAi JF02268 (II)* ($P = 0.9759$, $n = 2$), *Or47b-GAL4 UAS-nj-hp 12.3 RNAi (II)* ($P = 0.7745$, $n = 2$): *Or47b-GAL4 UAS-CamKI RNAi JF02268 (II)* ($P < 0.8685$, $n = 2$); *UAS-nj-hp 12.3 RNAi (II): Or47b-GAL4 UAS-nj-hp 12.3 RNAi (II)* ($P = 0.9173$, $n = 2$); *UAS-CamKI RNAi JF02268 (II): Or47b-GAL4 UAS-CamKI RNAi JF02268 (II)* ($P = 0.8438$, $n = 2$).

Figure S4

Figure S4A. p300; *UAS-met RNAi (II): Or47b-GAL4 UAS-met RNAi (II)* ($P = 0.0016$, $n = 2$); *Or47b-GAL4 UAS-gce RNAi (II)* ($P = 0.0064$, $n = 2$); *UAS-gce RNAi (II): Or47b-GAL4 UAS-met RNAi (II)* ($P = 0.0009$, $n = 2$); *Or47b-GAL4 UAS-gce RNAi (II)* ($P = 0.0029$, $n = 2$).

Figure S4B. H3K27ac; *UAS-gce RNAi (II): Or47b-GAL4 UAS-gce RNAi (II)* ($P = 0.6957$, $n = 2$).

Figure S1C. GH w^{1118} comparison: SH w^{1118} 180 whole antennae ($P = 0.3469$, n = 6).

Figure S1D. p300; *UAS-met RNAi (II): Or47b-GAL4 UAS-met RNAi (II)* ($P = 0.0008$, $n = 2$); *Or47b-GAL4 UAS-gce RNAi (II)* ($P = 0.0007$, $n = 2$); *UAS-gce RNAi (II): Or47b-GAL4 UAS-met RNAi (II)* ($P = 0.0036$, $n = 2$); *Or47b-GAL4 UAS-gce RNAi (II)* ($P = 0.0029$, $n = 2$).

Figure S1E. H3K27ac; *UAS-gce RNAi (II): Or47b-GAL4 UAS-gce RNAi (II)* ($P = 0.6957$, $n = 2$).

SUPPLEMENTARY MATERIAL

Supplementary material for this article is available at http://advances.sciencemag.org/cgi/content/full/6/21/eaba6913/DC1

View/request a protocol for this paper from *Bio-protocol*.

REFERENCES AND NOTES

1. B. S. Cushing, K. M. Kramer, Mechanisms underlying epigenetic effects of early social experience: The role of neuropeptides and steroids. *Neurosci. Biobehav. Rev.* **29**, 1089–1105 (2005).
2. S. Dey, P. Chamero, J. K. Pru, M.-S. Chien, X. Ibarra-Soria, K. R. Spencer, D. W. Logan, H. Matsunami, J. J. Peluso, L. Stowers, Cyclic regulation of sensory perception by a female hormone alters behavior. *Cell* **161**, 1334–1344 (2015).
3. R. Nardou, E. M. Lewis, R. Rothhaas, R. Xu, A. Yang, E. Boyden, G. Dölen, Oxytocin-dependent reopening of a social reward learning critical period with MDMA. *Nature* **569**, 116–120 (2019).
4. T. K. Hensch, Critical period regulation. *Annu. Rev. Neurosci.* **27**, 549–579 (2004).
5. B. J. Dickson, Wired for sex: The neurobiology of *Drosophila* mating decisions. *Science* **322**, 904–909 (2008).
6. D. Yamamoto, M. Koganezawa, Genes and circuits of courtship behaviour in *Drosophila* males. *Nat. Rev. Neurosci.* **14**, 681–692 (2013).
7. K. Sato, D. Yamamoto, The mode of action of Fruitless: Is it an easy matter to switch the sex? *Genes Brain Behav.* **19**, e12606 (2020).
8. A. Kurtovic, A. Widmer, B. J. Dickson, A single class of olfactory neurons mediates behavioural responses to a *Drosophila* sex pheromone. *Nature* **446**, 542–546 (2007).
9. H. K. Dweck, S. A. M. Ebrahim, M. Thoma, A. A. M. Mohamed, I. W. Keesey, F. Trona, S. Lavista-Llanos, A. Svatoš, S. Sachse, M. Knaden, B. S. Hansson, Pheromones mediating copulation and attraction in *Drosophila*. *Proc. Natl. Acad. Sci. U.S.A.* **112**, E2829–E2835 (2015).

10. S. Sethi, H.-H. Lin, A. K. Shepherd, P. C. Volkan, C.-Y. Su, J. W. Wang, Social context enhances hormonal modulation of pheromone detection in *Drosophila*. *Curr. Biol.* **29**, 3887–3898.e4 (2019).
11. H.-H. Lin, D.-S. Cao, S. Sethi, Z. Zeng, J. S. R. Chin, T. S. Chakraborty, A. K. Shepherd, C. A. Nguyen, J. Y. Yew, C.-Y. Su, J. W. Wang, Hormonal modulation of pheromone detection enhances male courtship success. *Neuron* **90**, 1272–1285 (2016).
12. L. Wang, X. Han, J. Mehren, M. Hiroi, J.-C. Billeter, T. Miyamoto, H. Amrein, J. D. Levine, D. J. Anderson, Hierarchical chemosensory regulation of male-male social interactions in *Drosophila*. *Nat. Neurosci.* **14**, 757–762 (2011).
13. C. E. Hueston, D. Olsen, Q. Li, S. Okuwa, B. Peng, J. Wu, P. C. Volkan, Chromatin modulatory proteins and olfactory receptor signaling in the refinement and maintenance of *Fruitless* expression in olfactory receptor neurons. *PLOS Biol.* **14**, e1002443 (2016).
14. S. Venkatesh, J. L. Workman, Histone exchange, chromatin structure and the regulation of transcription. *Nat. Rev. Mol. Cell Biol.* **16**, 178–189 (2015).
15. H. M. Chan, N. B. La Thangue, p300/CBP proteins: HATs for transcriptional bridges and scaffolds. *J. Cell Sci.* **114**, 2363–2373 (2001).
16. E. Kalkhoven, CBP and p300: HATs for different occasions. *Biochem. Pharmacol.* **68**, 1145–1155 (2004).
17. S. Barish, Q. Li, J. W. Pan, C. Soeder, C. Jones, P. C. Volkan, Transcriptional profiling of olfactory system development identifies *distal antenna* as a regulator of subset of neuronal fates. *Sci. Rep.* **7**, 40873 (2017).
18. N. Koike, S.-H. Yoo, H.-C. Huang, V. Kumar, C. Lee, T.-K. Kim, J. S. Takahashi, Transcriptional architecture and chromatin landscape of the core circadian clock in mammals. *Science* **338**, 349–354 (2012).
19. V. Tiwari, S. D. Karpe, R. Sowdhamini, Topology prediction of insect olfactory receptors. *Curr. Opin. Struct. Biol.* **55**, 194–203 (2019).
20. S. Impey, A. L. Fong, Y. Wang, J. R. Cardinaux, D. M. Fass, K. Obrietan, G. A. Wayman, D. R. Storm, T. R. Soderling, R. H. Goodman, Phosphorylation of CBP mediates transcriptional activation by neural activity and CaM kinase IV. *Neuron* **34**, 235–244 (2002).
21. G. P. Vicent, A. S. Nacht, R. Zaurín, C. Ballaré, J. Clausell, M. Beato, Minireview: Role of kinases and chromatin remodeling in progesterone signaling to chromatin. *Mol. Endocrinol.* **24**, 2088–2098 (2010).
22. K. Usui-Aoki, H. Ito, K. Ui-Tei, K. Takahashi, T. Lukacsovich, W. Awano, H. Nakata, Z. F. Piao, E. E. Nilsson, J. Tomida, D. Yamamoto, Formation of the male-specific muscle in female *Drosophila* by ectopic *fruitless* expression. *Nat. Cell Biol.* **2**, 500–506 (2000).
23. S. S. Lee, Y. Ding, N. Karapetians, C. Rivera-Perez, F. G. Noriega, M. E. Adams, Hormonal signaling cascade during an early-adult critical period required for courtship memory retention in *Drosophila*. *Curr. Biol.* **27**, 2798–2809.e3 (2017).
24. M. Bownes, H. Rembold, The titre of juvenile hormone during the pupal and adult stages of the life cycle of *Drosophila melanogaster*. *Eur. J. Biochem.* **164**, 709–712 (1987).
25. S. Barish, S. Nuss, I. Strunilin, S. Bao, S. Mukherjee, C. D. Jones, P. C. Volkan, Combinations of DIPs and Dprs control organization of olfactory receptor neuron terminals in *Drosophila*. *PLOS Genet.* **14**, e1007560 (2018).
26. W. J. Joo, L. B. Sweeney, L. Liang, L. Luo, Linking cell fate, trajectory choice, and target selection: Genetic analysis of Sema-2b in olfactory axon targeting. *Neuron* **78**, 673–686 (2013).
27. M. A. Mahajan, H. H. Samuels, Nuclear hormone receptor coregulator: Role in hormone action, metabolism, growth, and development. *Endocr. Rev.* **26**, 583–597 (2005).
28. K. J. Ferrari, A. Scelfo, S. Jammula, A. Cuomo, I. Barozzi, A. Stützer, W. Fischle, T. Bonaldi, D. Pasini, Polycomb-dependent H3K27me1 and H3K27me2 regulate active transcription and enhancer fidelity. *Mol. Cell* **53**, 49–62 (2014).
29. G. Dölen, A. Darvishzadeh, K. W. Huang, R. C. Malenka, Social reward requires coordinated activity of accumbens oxytocin and 5HT. *Nature* **501**, 179–184 (2013).
30. C. J. Fryer, T. K. Archer, Chromatin remodelling by the glucocorticoid receptor requires the BRG1 complex. *Nature* **393**, 88–91 (1998).
31. A. F. Trollope, M. Gutièrrez-Mecinas, K. R. Mifsud, A. Collins, E. A. Saunderson, J. M. H. M. Reul, Stress, epigenetic control of gene expression and memory formation. *Exp. Neurol.* **233**, 3–11 (2012).
32. I. C. G. Weaver, N. Cervoni, F. A. Champagne, A. C. D'Alessio, S. Sharma, J. R. Seckl, S. Dymov, M. Szyf, M. J. Meaney, Epigenetic programming by maternal behavior. *Nat. Neurosci.* **7**, 847–854 (2004).
33. P. O. McGowan, A. Sasaki, A. C. D'Alessio, S. Dymov, B. Labontè, M. Szyf, G. Turecki, M. J. Meaney, Epigenetic regulation of the glucocorticoid receptor in human brain associates with childhood abuse. *Nat. Neurosci.* **12**, 342–348 (2009).
34. E. Edsinger, G. Dölen, A conserved role for serotonergic neurotransmission in mediating social behavior in octopus. *Curr. Biol.* **28**, 3136–3142.e4 (2018).
35. K. R. Mifsud, M. Gutièrrez-Mecinas, A. F. Trollope, A. Collins, E. A. Saunderson, J. M. H. M. Reul, Epigenetic mechanisms in stress and adaptation. *Brain Behav. Immun.* **25**, 1305–1315 (2011).
36. M. C. Neville, T. Nojima, E. Ashley, D. J. Parker, J. Walker, T. Southall, B. Van de Sande, A. C. Marques, B. Fischer, A. H. Brand, S. Russell, M. G. Ritchie, S. Aerts, S. F. Goodwin, Male-specific fruitless isoforms target neurodevelopmental genes to specify a sexually dimorphic nervous system. *Curr. Biol.* **24**, 229–241 (2014).
37. M. Slattery, L. Ma, N. Négre, K. P. White, R. S. Mann, Genome-wide tissue-specific occupancy of the hox protein ultrabithorax and hox cofactor homothorax in *Drosophila*. *PLOS ONE.* **6**, e14686 (2011).
38. Q. Li, S. Barish, S. Okuwa, A. Maciejewski, A. T. Brandt, D. Reinhold, C. D. Jones, P. C. Volkan, A functionally conserved gene regulatory network module governing olfactory neuron diversity. *PLOS Genet.* **12**, e1005780 (2016).
39. C. K. Sim, S. Perry, S. K. Tharadra, J. S. Lipsick, A. Ray, Epigenetic regulation of olfactory receptor gene expression by the Myb-MuvB/dREAM complex. *Genes Dev.* **26**, 2483–2498 (2012).
40. T. Lilja, D. Qi, M. Stabell, M. Mannervik, The CBP coactivator functions both upstream and downstream of Dpp/Screw signaling in the early *Drosophila* embryo. *Dev. Biol.* **262**, 294–302 (2003).

Acknowledgments: We thank C. Jones for consultation on statistical analysis, and the members of the Volkan laboratory and Hiro Matsunami for help with the manuscript. We thank Corbin Jones, Sachin Sethi, and Jing Wang for discussions. We thank the Smolik, Desplan, Mannervik, and Nijhout laboratories for sharing reagents, as well as the Bloomington Stock Center, Drosophila Genetic Resource Center, Duke Light Microscopy Core Facility, Duke Microarray Core Facility, and UNC High-Throughput Sequencing Facility for services. **Funding:** This study was supported by National Institutes of Health grant number R01 NS109401 to P.C.V. **Author contributions:** S.Z., B.D., and P.C.V. designed the study. S.Z. and B.D. performed all experiments with the help of G.T.B. and P.G.S. Gce antibodies were generated by A.M.R. **Competing interests:** The authors declare that they have no competing interests. **Data and materials availability:** All data needed to evaluate the conclusions in the paper are present in the paper and/or the Supplementary Materials. Additional data related to this paper may be requested from the authors.

Submitted 23 December 2019
Accepted 18 March 2020
Published 22 May 2020
10.1126/sciadv.aba6913

Citation: S. Zhao, B. Deanhardt, G. T. Barlow, P. G. Schleske, A. M. Rossi, P. C. Volkan, Chromatin-based reprogramming of a courtship regulator by concurrent pheromone perception and hormone signaling. *Sci. Adv.* **6**, eaba6913 (2020).

Science Advances

Chromatin-based reprogramming of a courtship regulator by concurrent pheromone perception and hormone signaling

Songhui Zhao, Bryson Deanhardt, George Thomas Barlow, Paulina Guerra Schleske, Anthony M. Rossi and Pelin C. Volkan

Sci Adv **6** (21), eaba6913.
DOI: 10.1126/sciadv.aba6913

Science Advances (ISSN 2375-2548) is published by the American Association for the Advancement of Science, 1200 New York Avenue NW, Washington, DC 20005. The title *Science Advances* is a registered trademark of AAAS.